A ROLE FOR THE OUTER RETINA IN DEVELOPMENT OF THE INTRINSIC PUPILLARY LIGHT REFLEX IN MICE

A. VUGLER, [a]* M. SEMO, [a] A. ORTÍN-MARTÍNEZ, [b]
A. ROJANASAKUL, [a] B. NOMMISTE, [a]
F. J. VALIENTE-SORIANO, [b] D. GARCÍA-AYUSO, [b]
P. COFFEY, [a] M. VIDAL-SANZ [b] AND C. GIAS [a]

[a] *Department of Ocular Biology and Therapeutics, UCL-Institute of Ophthalmology, 11-43 Bath Street, London, UK*

[b] *Departamento de Oftalmología, Facultad de Medicina, Universidad de Murcia, and Instituto Murciano de Investigación Biosanitaria Virgen de la Arrixaca (IMIB-Arrixaca), Murcia, Spain*

Abstract—Mice do not require the brain in order to maintain constricted pupils. However, little is known about this intrinsic pupillary light reflex (iPLR) beyond a requirement for melanopsin in the iris and an intact retinal ciliary marginal zone (CMZ). Here, we study the mouse iPLR *in vitro* and examine a potential role for outer retina (rods and cones) in this response. In wild-type mice the iPLR was absent at postnatal day 17 (P17), developing progressively from P21–P49. However, the iPLR only achieved ∼30% of the wild-type constriction in adult mice with severe outer retinal degeneration (*rd* and *rdcl*). Paradoxically, the iPLR increased significantly in retinal degenerate mice >1.5 years of age. This was accompanied by an increase in baseline pupil tone in the dark to levels indistinguishable from those in adult wild types. This rejuvenated iPLR response was slowed by atropine application, suggesting the involvement of cholinergic neurotransmission. We could find no evidence of an increase in melanopsin expression by quantitative PCR in the iris and ciliary body of aged retinal degenerates and a detailed anatomical analysis revealed a significant decline in melanopsin-positive intrinsically photosensitive retinal ganglion cells (ipRGCs) in *rdcl* mice >1.5 years. Adult mice lacking rod function (*Gnat1*−/−) also had a weak iPLR, while mice lacking functional cones (*Cpfl5*) maintained a robust response. We also identify an important role for pigmentation in the development of the mouse iPLR, with only a weak and transient response present in albino animals. Our results show that the iPLR in mice develops unexpectedly late and are consistent with a role for rods and pigmentation in the development of this response in
mice. The enhancement of the iPLR in aged degenerate mice was extremely surprising but may have relevance to behavioral observations in mice and patients with retinitis pigmentosa. © 2014 The Authors. Published by Elsevier Ltd. on behalf of IBRO. This is an open access article under the CC BY license (http://creativecommons.org/licenses/by/3.0/).

Key words: melanopsin, development, *rd* mice, pigmentation, pupillary light reflex, retinitis pigmentosa.

INTRODUCTION

Pupil constriction is maintained during daylight hours by the pupillary light reflex (PLR), a neural pathway traditionally thought to involve input from different components of the retina, relay via midbrain nuclei and output to muscles of the iris via the ciliary ganglion (Alexandridis, 1985; Lucas et al., 2003; Guler et al., 2008; Lall et al., 2010; Chen et al., 2011). However, it has been known for some time now that the irises of fish and amphibians (Seliger, 1962; Barr and Alpern, 1963), birds (Tu et al., 2004) and some mammals, including rats (Bito and Turansky, 1975; Lau et al., 1992) can constrict in response to light independently of the brain.

Recently, it has been demonstrated in both anaesthetized and conscious preparations that mice also retain an intrinsic pupillary light reflex (iPLR) following axotomy (Xue et al., 2011; Semo et al., 2014). In both studies, the iPLR was sufficient to maintain pupil constriction over a range of physiologically relevant light intensities and was absent in adult mice lacking the melanopsin gene (*Opn4*−/−). In addition to a dependence upon melanopsin and phospholipase C β4 (Xue et al., 2011), the iPLR in mice requires cholinergic neurotransmission (Semo et al., 2014; Schmidt et al., 2014a) and is also inhibited by selective damage to the ciliary marginal zone (CMZ) of the retina (Semo et al., 2014).

In the mouse eye, melanopsin is expressed in the iris (Xue et al., 2011), ciliary body (Semo et al., 2014), retinal pigment epithelium (Peirson et al., 2004) and retina. In the retina, melanopsin is expressed by intrinsically photosensitive retinal ganglion cells (ipRGCs), a heterogeneous population of neurons sending axons to a variety of subcortical brain structures, including the midbrain olivary pretectal nucleus (OPN), which mediates the conventional PLR (Hattar et al., 2006; Baver et al., 2008; Chen et al., 2011). In addition to this, ipRGCs also send axonal collaterals up into the inner plexiform layer of the retina, which may mediate a novel form of retrograde visual

signaling (Zhang et al., 2012; Joo et al., 2013). In rodents, ipRGCs are more common in the superior and temporal retina (Hannibal et al., 2002; Hattar et al., 2002; Vugler et al., 2008; Galindo-Romero et al., 2013; Hughes et al., 2013; Nadal-Nicolas et al., 2014; Valente-Soriano et al., 2014), with a discrete, melanopsin-rich plexus in the extreme retinal periphery (CMZ) of rats and mice (Vugler et al., 2008; Semo et al., 2014). In the mouse CMZ, we have shown that Brn3b-negative melanopsin neurons send projections directly into the ciliary body (Semo et al., 2014), a finding which complements recent reports of a direct retinal projection from ipRGCs into the mouse iris (Schmidt et al., 2014a).

In addition to being intrinsically light responsive, ipRGCs also receive synaptic input from rods and cones (Dacey et al., 2005; Schmidt et al., 2008; Weng et al., 2013). The genetic elimination of ipRGCs has shown them to be required for non-image forming vision in mice (Guler et al., 2008) and the current thinking is that ipRGCs integrate rod and cone signals with their own melanopsin-driven light responses to control important aspects of non-image forming and image-forming vision (Lucas et al., 2003; Panda et al., 2003; Brown et al., 2010, 2012; Ecker et al., 2010; Estevez et al., 2012; Allen et al., 2014; Schmidt et al., 2014b).

To date, nothing is known about the development of iPLR in mice beyond an apparent requirement for melanopsin from birth. As such, we were keen to examine the time course of iPLR development in wild-type mice and to use mice lacking functional rods and cones to explore if melanopsin alone is sufficient for iPLR development. This appeared to be a sensible question to ask given the known routing of rod/cone signals through ipRGCs and emerging evidence of a direct retinal contribution to the iPLR. As our established intraocular axotomy procedure was not feasible on retinal degenerate mice (Semo et al., 2014), we chose to validate and use a new *in vitro* approach here.

Our new method proved to be a good way of studying the iPLR in mice, giving comparable results to previous *in vivo* experiments. In retinal degenerate mice the *in vitro* pupillometry was correlated with molecular analysis of melanopsin expression in iris/ciliary body and a detailed anatomical assessment of ipRGC survival. This revealed a paradoxical increase in the strength of the iPLR response in aged retinal degenerates that occurred in parallel with a significant decline in the number of melanopsin-positive ipRGCs.

EXPERIMENTAL PROCEDURES

Animals

All procedures were conducted according to the Home Office (UK) regulations, under the Animals (Scientific Procedures) Act of 1986 and associated guidelines, with local ethics committee approval. All animals were housed under a 12-h light, 12-h dark cycle (lights on at 07:00, lights off at 19:00), with food and water available *ad libitum*. The following strains/genotypes of mice were used in our experiments: wildtype C57BL/6 (Harlan, UK); wildtype C3H/He; mice lacking either rods (*rd/rd*) or rods

and cones (*rd/rd cl*), which are both on the C3H/He background; melanopsin knockout (*Opn4$^{-/-}$*) mice and triple knockout (*Opn4$^{-/-}$*, *Gnat1$^{-/-}$*, *Cnga3$^{-/-}$*) mice, which are both on a C57BL/6-129 mixed strain background (Hattar et al., 2003; Lucas et al., 2003); red cone knock-in (*Opn1mw^R*) mice which are on a C57BL/6 background (Lall et al., 2010) and were obtained from the colony maintained at the University of Manchester, UK; Cone photoreceptor function loss 5 (*Cpfl5*) mice (Pang et al., 2012), which are on a mixed C57BL/6 background; rod α-transducin knockout (*Gnat1$^{-/-}$*) mice which are on a mixed 129/Sv-BALB/c background (Calvert et al., 2000) and albino mice of either the BALB/c or MF1 strain (both from Harlan, UK). The mice used in our experiments were of mixed sex and ranged in age from postnatal day 17 (P17) to 30 months. Unless otherwise stated, all mice came from colonies maintained at UCL-Institute of Ophthalmology, UK.

In vitro pupillometry to isolate the iPLR

The methodology used here to isolate iPLR in mice is similar to that used for recording iPLRs from the isolated anterior chamber (Semo et al., 2014). However, instead of dissecting away the posterior segment, here we used a relatively simple whole-eye preparation to study pupillary constriction in the intact, isolated mouse eye. Following the initial experiments described in the sections 'Irradiance response under light and dark-adapted conditions' and 'Influence of stimulus duration on the dark-adapted iPLR', all subsequent experiments were carried out as described below in this section, with both eyes from a single mouse studied in darkness following a period of overnight dark adaptation. Occasionally, the PLR video acquisition software crashed and data from individual eyes were lost (hence the disparity between eye and animal numbers below).

On the morning of experimentation (between 08:00 and 11:00), mice were killed by cervical dislocation under red light. Eyes were removed with scissors and placed carefully (corneal surface upwards) onto on a custom-made Perspex indentation and covered with 4 drops of Neurobasal® culture medium (Invitrogen, 12348-017), which had been preheated to 37 °C. Eyes were illuminated with an infra-red light source and then stimulated with broad-spectrum white light originating from a xenon-arc lamp (Lambda DG-4, Linton Instrumentation). The stimulating light was heat filtered (preventing the passage of wavelengths > 600 nm) and then guided through a fiber optic cable, which terminated 1.5 cm away from the cornea, delivering 63 mW/cm^2 to the eye. The iPLR was recorded under infrared illumination, with 30 s of baseline recording in darkness followed by 60 s of light stimulation and a further 60 s of post-stimulation recording.

As described previously (Semo et al., 2010, 2014), pupil area was measured off-line at 1-s intervals by an observer using bespoke MATLAB software, with all iPLR measurements expressed as normalized pupil area (relative to the baseline pupil area). The baseline pupil area was also estimated in mm^2 following the calibration of video images using a scale bar placed at the level of

the eye. Results were expressed as % pupil area relative to adult wild-type mice. The following sections describe specific details for the individual experiments conducted in this study.

Irradiance response under light and dark-adapted conditions. As retinal function in mice is enhanced by darkness (Fan et al., 2003) and the conventional PLR is routinely recorded following a period of dark adaptation (Lucas et al., 2003; McNeill et al., 2011), we initially sought to examine the influence of this variable on the strength of iPLR recordings in wildtype adult mice. For this experiment, two groups of C3H/He mice (6–9 months old) were either fully light adapted (lights on at 07:00 and recordings conducted under ambient illumination between 13:00 and 15:00) or dark-adapted over night prior to recordings in darkness between 08:00 and 11:00 the following morning. Before the light-adapted recordings, irradiance levels at cage and Perspex eye holder were $\sim$8.7 μW/cm^2 and $\sim$14.7 μW/cm^2 respectively. Following 30 s of baseline recording (in darkness or ambient illumination as appropriate), white light stimulation (60 s duration) was delivered to both light and dark-adapted eyes at irradiances of 63 μW, 630 μW, 6.3 mW or 63 mW/cm^2, produced using appropriate neutral density filters. Following cessation of the stimulus, a further 60 s of video footage was recorded for each eye (in darkness or ambient illumination as appropriate). The number of mice per irradiance group ranged between 4 and 8 and only one eye was stimulated per mouse.

Influence of stimulus duration on the dark-adapted iPLR. From the experiments described in the section 'Irradiance response under light and dark-adapted conditions', it became apparent that the recovery (post-stimulation phase) of the iPLR response was very slow. One possibility here is that the exposure to 60 s of bright light may have somehow saturated the response. So, in order to test this hypothesis and to further elucidate the temporal dynamics of iPLR in mice, we conducted an additional experiment, in which the excised eyes of dark-adapted wildtype mice were exposed to stimuli of constant intensity (63 mW/cm^2) but varying duration. There were 4 experimental groups: 10 ms, 50 ms, 100 ms, 500 ms and 1 s, with $n = 4$ eyes from $n = 4$ C3H/He mice (6–7 months old) per group. Each trial consisted of a 30-s pre-stimulation baseline recording component and 90 s of post-stimulation recording in darkness.

Intra-animal consistency of eye recordings. Following the results of experiments in 'Irradiance response under light and dark-adapted conditions' and 'Influence of stimulus duration on the dark-adapted iPLR', we decided to conduct all subsequent experiments under conditions that produced the most robust iPLR responses in wildtype mice (overnight dark-adaptation, with stimulation at 63 mW/cm^2 for 60 s). As we had limited numbers of retinal degenerate/genetically altered mice available, we next sort to validate a method by which we could analyze the iPLR from both eyes of a

single mouse. To this end, we conducted an experiment using 5 wildtype C3H/He mice (7–9 months old) in which the iPLR response of the first eye extracted was compared to that from the second eye. The eyes were prepared and stimulated according to the general method described above in the section 'Influence of stimulus duration on the dark-adapted iPLR' and for each animal, it took approximately 11 min (from death) to complete both iPLR recordings.

Influence of atropine and melanopsin on the in vitro iPLR. We have recently shown that both cholinergic neurotransmission and melanopsin are required for full expression of the iPLR response in conscious mice (Semo et al., 2014). In order to determine if our new *in vitro* preparation displayed similar characteristics, we recorded the iPLR from C3H/He wildtype mice ($n = 6$ eyes from $n = 4$ mice, aged 7–9 months old) that had received bilateral atropine drops as follows: 1 drop of 1% Minims atropine sulfate (preservative free) per eye, applied 30 min prior to cervical dislocation. We also recorded iPLR responses from $Opn4^{-/-}$ mice ($n = 7$ eyes from $n = 4$ mice, aged 9 months) and triple knockout mice ($n = 8$ eyes from $n = 4$ mice, aged 9 months), which lack melanopsin ($Opn4^{-/-}$), scotopic rod function ($Gnat1^{-/-}$) and functional cones ($Cnga3^{-/-}$). Again, all animals were dark-adapted overnight prior to recordings with 60-s light stimulation at 63 mW/cm^2.

Development of the iPLR in wildtype mice. The time course of iPLR development was studied in wildtype C57BL/6 mice over the first 7 weeks of postnatal life. Initially, we chose to examine the iPLR at P17 ($n = 5$ eyes from $n = 4$ mice), a time point at which the eyelids have been open for several days and the conventional PLR is fully developed (McNeill et al., 2011). Subsequently, we examined development of the iPLR response in older mice at P49 ($n = 8$ eyes from $n = 4$ mice), P24 ($n = 7$ eyes from $n = 4$ mice) and P21 ($n = 6$ eyes from $n = 4$ mice). In addition to the C57BL/6 mice, we also examined iPLR responses in young C3H/He wildtype mice at P17 ($n = 10$ eyes from $n = 6$ mice) and P35 ($n = 6$ eyes from $n = 4$ mice). We were also able to examine the iPLR in aged C3H/He wildtype mice ($n = 6$ eyes from $n = 3$ mice, aged 23 months). All mice were dark-adapted overnight prior to recordings with 60-s light stimulation at 63 mW/cm^2.

Development of the iPLR in mice lacking functional rods and cones. In order to determine the extent to which melanopsin is responsible for iPLR development in mice, we studied this phenomenon in adult animals that lack rods (*rd/rd*), or both rods and cones (*rd/rd cl*). As these animals came from the same breeding colony, *rd/rd* and *rd/rd cl* mice were distinguished from each other by genotyping prior to iPLR recordings. The mice used in this experiment ranged in age from 7 to 30 months, with both *rd/rd* (abbreviated to *rd*) and *rd/rd cl* (abbreviated to *rdcl*) mice being further subdivided into two groups classified as "adult" (7–9 months old) and "aged" (20–30 months old).

The number of eyes recorded per group was as follows: adult *rd* (*n* = 12 eyes from *n* = 6 mice), aged *rd* (*n* = 8 eyes from *n* = 4 mice), adult *rdcl* (*n* = 8 eyes from *n* = 4 mice), aged *rdcl* (*n* = 9 eyes from *n* = 5 mice). Another group of adult *rd* mice (*n* = 7 from *n* = 4 mice) and aged *rd* mice (*n* = 6 eyes from *n* = 3 mice) received topical atropine drops 30 min prior to iPLR recordings using the method detailed in Section 'Influence of atropine and melanopsin on the in vitro iPLR' above. In addition to adult and aged mice, we also recorded iPLR responses from P17 mice (mixed *rd* and *rdcl* mice, *n* = 14 eyes from *n* = 8 animals). Following iPLR recordings from *rd* and *rdcl* mice, eyes were frozen, sectioned and stained with DAPI in order to confirm retinal degeneration.

In addition to *rd* and *rdcl* mice, which exhibit rapid rod and cone degeneration over the first three postnatal weeks (Soucy et al., 1998; Strettoi et al., 2002), we were also able to record iPLR responses from adult *Gnat1*$^{-/-}$ mice (2 months old, *n* = 6 eyes from *n* = 3 mice), which lack all scotopic rod function from birth but undergo a slow rod degeneration (Calvert et al., 2000) and adult *Cpfl5* mice (4–7 months old, *n* = 13 eyes from *n* = 7 mice), which lack all cone function from birth and exhibit a slow, regionally specific loss of cones (Pang et al., 2012). Interestingly, these animals displayed various levels of pigmentation in their coats, with the *Gnat1*$^{-/-}$ mice all appearing a light caramel color and the *Cpfl5* mice being composed of a mixture of black (*n* = 4 mice) and agouti (*n* = 3 mice) litter mates. In light of this observation and the iPLR results obtained, we examined the variable of pigmentation further by recording responses from two strains of non-pigmented albino mice. These were BALB/c (2 months old, *n* = 8 eyes from *n* = 4 mice) and MF1 mice (3 months old, *n* = 7 eyes from *n* = 4 mice).

Preferential retinal stimulation using Opn1mw^R mice. In light of growing evidence suggesting the existence of a direct projection from ipRGCs into the ciliary body/iris (Rupp et al., 2013; Semo et al., 2014; Schmidt et al., 2014a), we sought to determine if retinal stimulation alone could drive an iPLR response in mice. To do this we used *Opn1mw^R* mice (a kind gift from Prof. Robert Lucas at the University of Manchester, UK), in which the murine m-cone opsin is replaced with a coding sequence for the human red cone opsin (Smallwood et al., 2003). Due to the enhanced long wavelength sensitivity of the medium wavelength cones in these transgenic mice, exposure of the retina to red light now stimulates cones to a greater extent than melanopsin (Brown et al., 2012). As mouse cones are electrically coupled to rods via gap junctions (Asteriti et al., 2014) and ipRGCs receive both cone and rod inputs (Schmidt and Kofuji, 2010; Weng et al., 2013), we hypothesized that a greater degree of retinal activation (as opposed to iridial activation driven solely by melanopsin in the iris/ciliary body) could be achieved by exposing isolated *Opn1mw^R* mouse eyes to intense red light.

For this experiment, the *Opn1mw^R* mice (*n* = 4, aged 3 months, genotyped at the University of Manchester)

and C57BL/6 wildtype mice (*n* = 4 aged 3 months) were dark-adapted overnight prior to iPLR recordings between 08:00 and 11:00 the following day. Due to the red-light sensitivity of the *Opn1mw^R* mice, these animals were killed and their eyes removed in darkness using NVG-2 night vision goggles. This procedure was difficult and several eyes were discarded following failure to achieve proper orientation under night-vision conditions.

The iPLR responses (*n* = 6 eyes from *Opn1mw^R* mice and *n* = 6 eyes from wild-type mice) were then recorded and analyzed as described in the section 'The *in vitro* iPLR requires cholinergic neurotransmission and melanopsin', with the exception of the light stimulus, which was restricted to red light of 625–650 nm generated using appropriate filters. This red light was as bright as our system would allow, with irradiance of approximately 1.2×10^{16} photons/cm^2/s at the level of the eye preparation. Following iPLR recordings under red light stimulation, the eyes from *Opn1mw^R* mice were maintained in darkness for a further 2 min and then subsequently exposed to intense blue light (447-nm filter with a 60-nm bandwidth at $\sim2.9 \times 10^{14}$ photons/cm^2/s) in order to confirm the ability of these eyes to undergo iPLR.

Laser capture microdissection (LCMD) and quantitative real-time PCR

In order to examine the influence of age and retinal dystrophy on melanopsin expression in iris and ciliary body of *rd* mice, we performed LCMD on four groups: adult *rd* mice (7–8 months old, *n* = 8 eyes from *n* = 4 mice), aged *rd* mice (22–23 months old, *n* = 8 eyes from *n* = 4 mice), adult C3H/He wildtype mice (7–8 months old, *n* = 8 eyes from *n* = 4 mice) and aged C3H/He wildtype mice (22 months old, *n* = 8 eyes from *n* = 4 mice). The eyes were collected in a counterbalanced fashion under ambient laboratory illumination between the hours of 09:00–11:00. For each mouse, following death by cervical dislocation, both eyes were rapidly frozen in OCT embedding compound.

Eye sections were then cut on a cryostat (25-μm thick) and mounted onto MembraneSlides NF 1.0 PEN (Carl Zeiss Ltd., UK). Sections of iris or ciliary body were laser dissected with a PALM microbeam laser (P.A.L.M. Microlaser Technologies AG, Beinried, Germany) running Microlaser systems 3.1 Robosoftware. Microdissected tissues were collected into adhesive caps (Carl Zeiss), with tissue from the 8 eyes in each group pooled into one sample per group, which contained approximately 32 pieces of iris or ciliary body.

Total RNA was extracted using an RNeasy micro extraction kit following the manufacturers protocol for laser-microdissected cryosections (Qiagen, Crawley UK). This total RNA was then DNase treated to remove genomic contamination (DNase I, Amplification grade Invitrogen (Life Technologies Carlsbad, CA USA)) and then reverse transcribed into cDNA using SuperScript® III First-Strand Synthesis SuperMix for qRT-PCR (Life Technologies) following the manufacturers protocol.

In addition to melanopsin, we also chose to examine the gene expression for rhodopsin, which has also been

reported in mammalian iris (Ghosh et al., 2004; Xue et al., 2011). Melanopsin and rhodopsin primers were designed using the Primer3 algorithm, and TATA-binding protein (TBP) primers were as described previously (Semo et al., 2003b). These primers produce intron-spanning products, preventing genomic DNA amplification and all primers used produced a single product, confirmed by melting curve analysis that was sequenced to confirm identity. Two isoforms of melanopsin have been identified in mouse retina (Pires et al., 2009) and the primers designed here will amplify the same size product from both isoforms. The primer sequences used are detailed in Table 1.

Reactions were carried out using Power SYBR® Green on a 7900HT Fast Real Time PCR System (Applied Biosystems CA, USA). Each reaction was carried out in triplicate (providing technical replicates) and contained 300 nM of each primer with 5 µl of cDNA. Cycling conditions consisted of an initial *Taq* activation step of 95 °C for 10 min, followed by 40 cycles of 95 °C denaturation for 15 s followed by a 60 °C annealing/extension step for 1 min. A final data collection step of 30 s was added to each cycle, with fluorescence measured at 2 °C below the melting temperature of the desired product as determined by melting curve analysis, ensuring that primer-dimers did not contribute to measured fluorescence.

Real-time PCR data were analyzed using Data Analysis for Real-time PCR (Peirson et al., 2003). The slope of each amplification plot was used to calculate reaction efficiency and expression of each sample was then calculated from threshold cycle values as efficiency corrected relative expression (Pfaffl, 2001). TBP was used as an internal control, this gene has been shown to be expressed at stable levels in aging mouse eyes (Semo et al., 2003a,b).

Immunohistochemistry

Retinal whole mounts were obtained from *rdcl* and congenic wildtype C3H/He mice ranging in age from 1 to 2.5 years of age. This was done using our previously described methods (Vugler et al., 2008; Salinas-Navarro et al., 2009). Briefly, the animals were deeply anaesthetized and perfused with 0.1 M PBS followed by 4% paraformaldehyde. Eyes from each animal were then post-fixed for 2 h prior to removal of the retina. Orientation

Table 1. List of primer sequences used for detection of melanopsin and rhodopsin by quantitative real time PCR. Internal control gene was TATA-binding protein (TBP)

Gene of interest	Forward and reverse primers used
Melanopsin	Forward: GGGATGCTGGGCAATCTGAC Reverse: GTCGCTGACTGCGAGGTTGA
Rhodopsin	Forward: TCCATGCTGGCAGCGTACAT Reverse: GGACCACAGGGCGATTTCAC
TBP	Forward: TGGGCTTCCCAGCTAAGTTC Reverse: GGAAATAATTCTGGCTCATAGCTACTG

of whole mounts was achieved using the nasal caruncle and dorsal eyelid as reference points to make 1 large cut in the superior retina and three smaller cuts in the nasal, temporal and inferior retina of each eye. The ciliary marginal zone (CMZ) region was removed in its entirety where possible by gradually sliding a pair of closed microsurgical tweezers under the retinal periphery (this technique was less effective in the eyes from older animals where the retina was extremely thin). Vitreous was removed with filter paper and retinas were washed in 0.1 M PBS prior to immunohistochemistry.

Retinal whole mounts were processed concurrently for the detection of ipRGCs using a rabbit anti-melanopsin antibody (UF006, Advanced Targeting Systems, San Diego, US) and the general RGC population using a goat antibody raised against Brn3a (C-20, sc-31984, Santa Cruz). The Brn3a marker has been previously validated for detection of RGCs and only labels a tiny fraction of ipRGCs in rodents (Nadal-Nicolas et al., 2009; Galindo-Romero et al., 2013). For double labeling, retinas were first blocked for 2 h in 5% normal donkey serum (NDS) in 0.1 M PBS with 3% Triton, followed by overnight incubation with a cocktail containing the two primary antibodies (UF006 at 1:5000 and anti-Brn3a at 1:200, both diluted in 0.1 M PBS with 3% Triton and 1% NDS). The whole mounts were then washed in PBS and incubated for 2 h in TRITC-labeled anti-rabbit and FITC-labeled anti-goat secondary antibodies (Jackson ImmunoReseach, 1:200 in 0.1 M PBS containing 2% NDS and 0.3% Triton) before further washing in PBS, mounting and cover-slipping as previously described (Vugler et al., 2008). The right retina from one 8-month-old *rdcl* mouse was processed for melanopsin alone, while the left retina was processed in the absence of melanopsin primary antibody as a negative control.

Image analysis

Retinal whole mounts were re-constructed in their entirety according to previously described methods (Galindo-Romero et al., 2013; Ortin-Martinez et al., 2014). To achieve this, a series of images were acquired using an epifluorescence microscope (Axioscop 2 Plus; Zeiss Mikroskopie, Jena, Germany) equipped with a computer-driven motorized stage (ProScan H128 Series; Prior Scientific Instruments, Cambridge, UK) controlled by image analysis software (Image-Pro Plus, IPP 5.1 for Windows; Media Cybernetics, Silver Spring, MD). Reconstructed whole mounts, made up of 154 individual frames, were further processed using a graphics-editing program, when required (Adobe Photoshop CS 8.0.1; Adobe Systems, Inc., San Jose, CA).

Immunohistochemical staining was also analyzed using Zeiss LSM 510 and LSM 710 confocal microscopes with associated Zeiss image analysis software. The right retina from an 8-month-old *rdcl* mouse was also imaged in its entirety using the intelligent tiling function on the Zeiss 710 microscope.

Quantification and topographic analysis of ipRGCs and Brn3a. Briefly, the individual fluorescent images taken for each retinal whole-mount were processed by a specific subroutine using the IPP macro language. After

quantification, Brn3a$^+$RGC isodensity maps were constructed through a quadrant analysis as previously described in detail (Nadal-Nicolas et al., 2009; Galindo-Romero et al., 2013). Individual ipRGCs were dotted manually onto the retinal photomontage. Then, dots were automatically quantified and their retinal position extracted using the IPP macro language following previously described methods (Galindo-Romero et al., 2013).

In brief: after marking the optic nerve as a reference point and drawing the retinal contour, the number of dots representing ipRGCs and their x, y positions with respect to the optic nerve were calculated with a specific routine using the IPP macro language. All data (optic nerve coordinates, total number of cells and their retinal position) were exported to a spreadsheet (Office Excel 2000; Microsoft Corp., Redmond, WA). Retinal distribution of ipRGCs was then visualized using the k-nearest neighbor algorithm using a Java (Oracle Corporation, Redwood Shores, California, USA) application, as described previously (Galindo-Romero et al., 2013). Briefly, those cells within a fixed radius of 200 μm were counted as neighbors. Each ipRGC was then color-coded with a scale ranging from purple (0 neighbors) to red (11 or more neighbors).

Statistical analysis

All data were analyzed using GraphPad Prism software (GraphPad Software, San Diego, CA), with comparisons of pupil constriction over the duration of recordings made using a two-way repeated measures analysis of variance (ANOVA) followed by Bonferroni post hoc tests. In all repeated measures ANOVAs the subjects significantly matched ($P < 0.0001$). Peak constriction levels, latencies and baseline pupil areas were analyzed using one-tailed t-tests or a one-way ANOVA followed by Bonferonni's multiple comparison tests as appropriate. Cell count data were analyzed using a two-way and a one-way ANOVA followed by Bonferonni's post hoc tests.

RESULTS

Dark adaptation and increasing stimulus duration enhance the iPLR response

As shown in Fig. 1, using our simple *in vitro* technique, we were able to measure irradiance response relationships under light-adapted and dark-adapted conditions. Under ambient illumination (Fig. 1A), there was a significant effect of time $P < 0.0001$ ($F_{26,624} = 35.15$), irradiance $P < 0.001$ ($F_{3,624} = 38.01$) and a significant interaction between these two variables $P < 0.0001$ ($F_{78,624} = 16.45$) by 2-way ANOVA. Post hoc analysis revealed that no significant pupil constriction occurred below a stimulus intensity of 630 μW/cm^2 in the light-adapted eyes. However, peak constriction (measured by the lowest normalized pupil area obtained) was significantly increased between 630 μW/cm^2 and 6.3 mW/cm^2 ($P < 0.001$) under these conditions, with normalized pupil areas of 0.94 ± 0.01 and 0.80 ± 0.02 respectively. The peak constriction increased again between 6.3 mW/cm^2 and 63 mW/cm^2 (from 0.80 ± 0.02

to 0.58 ± 0.04, $P < 0.001$), with pupils being significantly more constricted at the highest light intensity both during and after the stimulation period (5–90 s, $P < 0.05$).

In comparison to the light-adapted iPLR, the dark-adapted response was far more sensitive (Fig. 1B), with a slow but noticeable decrease in normalized pupil area seen at the lowest stimulus intensity used (63 μW/cm^2). Under dark-adaptation, there was a significant effect of time $P < 0.0001$ ($F_{26,520} = 113.3$), irradiance $P < 0.001$ ($F_{3,520} = 10.35$) and a significant interaction between these two variables $P < 0.0001$ ($F_{78,520} = 15.71$) by a 2-way ANOVA. By post hoc analysis, the peak constriction was significantly increased between 63 μW/cm^2 and 630 μW/cm^2 ($P < 0.01$), with normalized pupil areas of 0.83 ± 0.04 and 0.55 ± 0.05 respectively. There were no significant differences between the dark-adapted iPLR at 630 μW/cm^2 and 6.3 mW/cm^2, with the strongest pupil constrictions seen in response to 63 mW/cm^2 (normalized pupil area of 0.37 ± 0.04). At this highest irradiance level, post hoc analysis revealed that the pupils were only significantly more constricted than those in the 6.3 mW/cm^2/630 μW/cm^2 groups during the initial phase of light stimulation (5–30 s, $P < 0.05$). Increasing the stimulus intensity under dark-adapted conditions significantly reduced the time to peak constriction (from 77.00 ± 10.52 s to 21.38 ± 5.90 s, $P = 0.0001$). Given that dark-adaptation and a stimulus intensity of 63 mW/cm^2 produced the strongest iPLR response in isolated mouse eyes, we decided to perform all subsequent experiments using these optimal conditions.

When studying the temporal dynamics of the iPLR under these optimized conditions we found a significant effect of time $P < 0.0001$ ($F_{26,390} = 42.36$), stimulus duration $P < 0.0001$ ($F_{3,390} = 28.02$) and a significant interaction between these two variables $P < 0.0001$ ($F_{104,390} = 7.378$) by a 2-way ANOVA (Fig. 1C). Rather surprisingly, there was a clear event-related decrease in normalized pupil area after just 50 ms of light stimulation (compare the first 15 s of response to 10-ms and 50-ms stimuli in Fig. 1C). This event-related response was also seen using the 100-ms stimulus but we could find no difference in iPLR response between 50 ms and 100 ms (100-ms data not shown). However, post hoc analysis confirmed a statistically significant decrease in normalized pupil area between 50 ms and 1 s (0.87 ± 0.03 verses 0.57 ± 0.02, $P < 0.001$). Importantly, the iPLR response appeared to display the same characteristics of a sustained constriction / slow recovery phase regardless of stimulus duration (compare Fig. 1B and Fig. 1C).

Given that the peak constriction was strongest in response to 60 s of illumination and because the iPLR is thought to function to sustain pupil constriction in mice (Xue et al., 2011), we chose to conduct all subsequent experiments using 60 s of light stimulation. This stimulus duration is also consistent with that used previously for recording iPLR responses in conscious mice (Semo et al., 2014). As shown in Fig. 1D, using 60-s stimulation at 63 mW/cm^2 irradiance in dark-adapted mice, we could find no statistically significant difference between iPLR
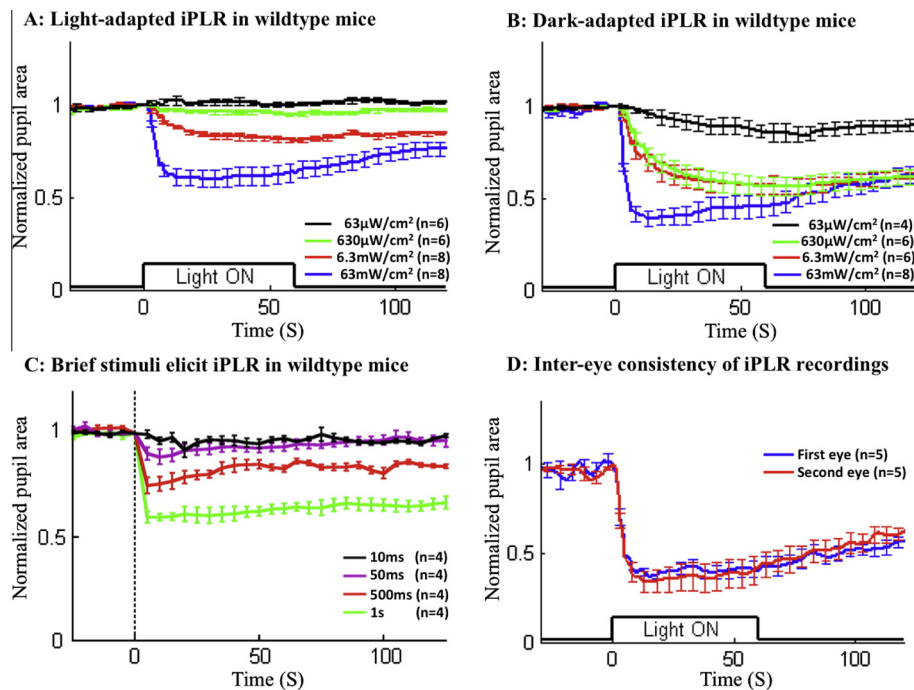
Fig. 1. Influence of dark adaptation, stimulus duration and sequence of intra-animal eye extraction on iPLR recordings from isolated mouse eyes. There was an irradiance response relationship under both light-adapted (A) and dark-adapted (B) conditions. An iPLR response can be elicited by 50 ms of light but increases in strength up to 1 s (C). The dotted line in C indicates stimulus onset. Note how even brief stimuli of 500 ms result in a sustained constriction response (C). (D) The high degree of inter-eye consistency when recording from both eyes of the same mouse. (B–D) Conducted under dark-adapted conditions. (C, D) Use an irradiance of 63 mW/cm^2. Data points are the mean ± SEM and "*n*" = total number of eyes examined.

recordings taken from the first and second eye of the same animal at any time point post-stimulation (Fig. 1D). Consequently, where possible, all subsequent experiments made use of both eyes from each mouse.

The *in vitro* iPLR requires cholinergic neurotransmission and melanopsin

Following topical atropine application to wildtype mice (Fig. 2A), we observed a significant increase in the latency to peak constriction in atropine-treated verses untreated eyes (80.33 ± 6.40 s verses 25.20 ± 6.51 s, $P < 0.0001$). However, this slower response reached similar peak constriction in both groups (0.32 ± 0.03 atropine-treated and 0.31 ± 0.03 untreated, non-significant, $P = 0.39$). By a 2-way ANOVA there was a significant interaction between time and atropine application $P < 0.0001$ ($F_{26,364} = 24.13$), with post hoc analysis confirming that atropine-treated pupils were significantly larger than untreated pupils during the initial post-stimulation phase. Interestingly, unlike the untreated group, atropine-treated pupils maintained their constriction at a constant level until cessation of recordings (Fig. 2A). This difference was significant by post hoc analysis, with the atropine-treated pupils being significantly smaller at 110 s ($P < 0.05$) and 120 s ($P < 0.01$) post-stimulation.

Given the results of previous studies (Xue et al., 2011; Semo et al., 2014), we hypothesized that the iPLR would be completely absent in the eyes of $Opn4^{-/-}$ mice. This was indeed the case in both $Opn4^{-/-}$ mice (Fig. 2B) triple

knockout ($Opn4^{-/-}$, $Gnat1^{-/-}$, $Cnga3^{-/-}$) mice (data not shown). Both the absence of a response in $Opn4^{-/-}$ mice and the dependence of iPLR latency on cholinergic neurotransmission are key characteristics of the iPLR in conscious animals (Semo et al., 2014). These findings serve to further validate our *in vitro* preparation while also underlining the fact that melanopsin expression is required for the development of iPLR in mice. Interestingly, our *in vitro* approach also reveals for the first time that cholinergic neurotransmission is required for the recovery phase of this response.

Development of the iPLR in wildtype mice

Fig. 3 shows the time course of iPLR development in wildtype (C57BL/6) mice. We found a significant effect of time $P < 0.0001$ ($F_{26,572} = 28.61$), age $P < 0.0001$ ($F_{3,572} = 56.30$) and a significant interaction between age and time $P < 0.0001$ ($F_{78,572} = 16.97$) by a 2-way ANOVA. Quite surprisingly, we could detect no iPLR response at P17 (Fig. 3A), a stage when the conventional PLR is already fully developed in mice (McNeill et al., 2011).

A clear, event-related response was first seen at P21 but this was small and lacked a sustained constriction phase (Fig. 3B). Post hoc analysis confirmed a significant difference in the iPLR response between P21 and P24 ($P < 0.01$). At P24, the response was strong (peak constriction of 0.63 ± 0.05 compared to 0.86 ± 0.05 at P21) and sustained, being significantly more constricted at P24 than P21 from 10 to 90 s
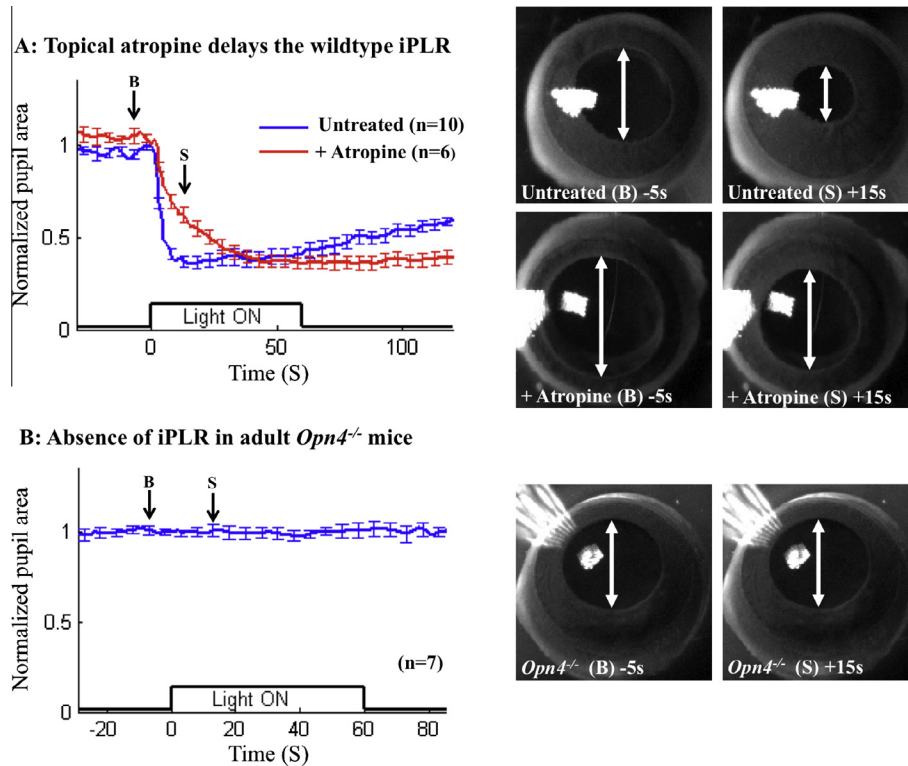
Fig. 2. The iPLR requires cholinergic neurotransmission and melanopsin. Atropine increases latency to peak constriction and sustains the constriction relative to untreated wild-type mice of the same strain (A). The iPLR was completely absent in $Opn4^{-/-}$ mice (B). Representative video stills are shown to the right, with baseline (B) and stimulated (S) corresponding to arrows on the associated graph. Data points are the mean ± SEM and "*n*" = total number of eyes examined. All eyes were dark-adapted prior to stimulation with 60 s of white light at 63 mW/cm^2. For clarity, double-headed arrows indicate the relative size of each pupil.

post-stimulation ($P < 0.05$). Between P24 and P49 the iPLR continued to get stronger (Fig. 3C), with a peak constriction of 0.23 ± 0.03 at P49. The constriction at P49 had the sustained constriction and slow recovery phase characteristic of adult eyes and was significantly greater than that at P24 at every time point analyzed from 5-s post-stimulation to the termination of recordings ($P < 0.01$). There was no significant difference in the latency to peak constriction between P24 and P49.

In addition to the C57BL/6 mice, we also studied the iPLR in C3H/He wildtype mice at P17 ($n = 10$ eyes) and P35 ($n = 6$ eyes). This strain of mouse displayed the same phenomenon, with an absence of iPLR at P17 and a robust response by P35 (data not shown).

Normal development of the iPLR requires an intact outer retina during early postnatal life

Given that the iPLR requires melanopsin from birth in order to develop (Fig. 2B), we next sought to determine if melanopsin alone drives iPLR development or whether rods and cones also contribute to the maturation of this response in mice. To address this issue we examined the iPLR in adult C3H/He mice with inherited rod degeneration that occurs either alone (*rd*) or in combination with the genetic ablation of cones (*rdcl*)

over the first three postnatal weeks (Soucy et al., 1998; Strettoi et al., 2002).

The adult mice used here ranged in age from 7 to 30 months and to our complete amazement we observed two different types of response dependent on the animal's age. In both the *rd* (Fig. 4A) and *rdcl* (Fig. 4B) mice, the iPLR was severely deficient in adults (aged 7–9 months), with a comparable small response also seen at P17 in *rd* and *rdcl* mice ($n = 14$ eyes, data not shown). However, as shown in Fig. 4A, B, to our complete surprise, the iPLR appeared relatively normal in aged *rd* and *rdcl* mice (aged 20–30 months). For the *rd* mice, there was a significant effect of time $P < 0.0001$ ($F_{17,306} = 23.89$), age $P < 0.01$ ($F_{1,306} = 10.87$) and an interaction between time and age $P < 0.0001$ ($F_{17,306} = 6.996$) by a 2-way ANOVA. There was a significant increase in peak constriction from 0.82 ± 0.02 in adults to 0.50 ± 0.08 in the aged mice ($P = 0.0001$), with a significant difference between the two constrictions at all post-stimulation time points analyzed.

The results of statistical analysis were similar for the *rdcl* mice, with a significant effect of time $P < 0.0001$ ($F_{16,240} = 43.74$), age $P < 0.0001$ ($F_{1,240} = 43.41$) and an interaction between time and age $P < 0.0001$ ($F_{16,240} = 16.16$) by a 2-way ANOVA. In these animals, the constriction increased in strength from a peak of
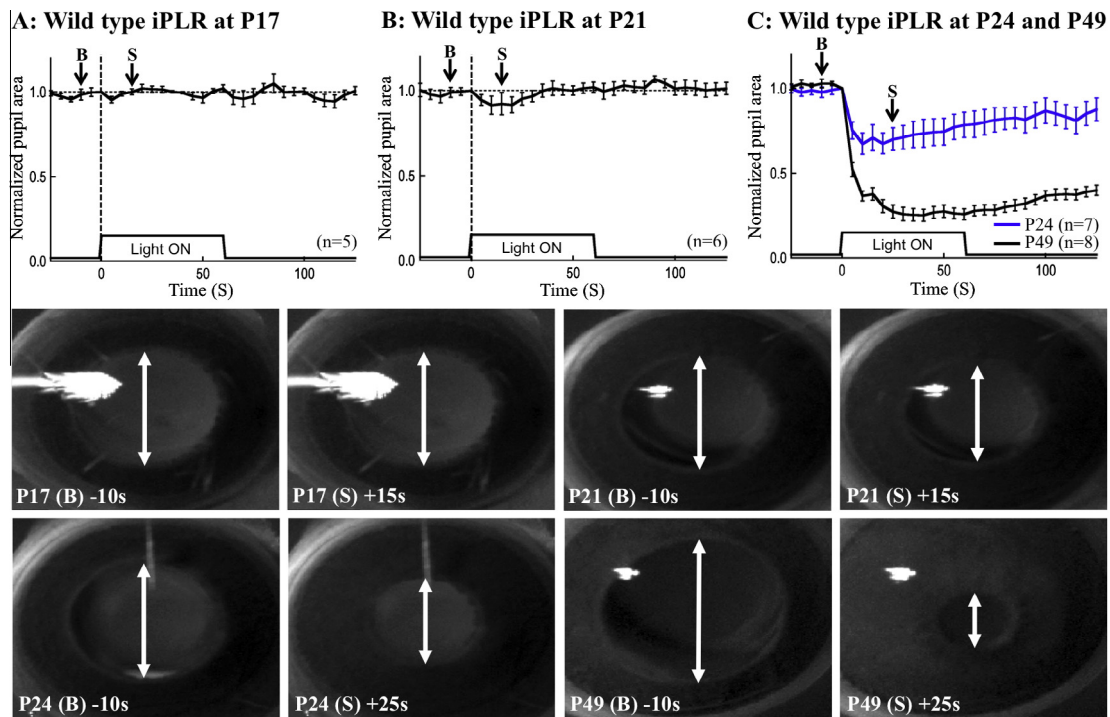
Fig. 3. The iPLR in wild-type mice develops after the third postnatal week. iPLR was absent in eyes from postnatal day 17 (P17) mice (A), with a small, event-related response first detected at P21 (B). At P24, light stimulation produced a larger, more sustained constriction, which increased in strength further still by P49 (C). Representative stills from video recordings are shown sequentially below the graphs, with baseline (B) and stimulated (S) corresponding to arrows on the associated graph. Data points are the mean ± SEM and "n" = total number of eyes examined. Eyes were dark-adapted prior to stimulation with 60 s of white light at an irradiance of 63 mW/cm^2. For clarity, double-headed arrows indicate the relative size of each pupil.

0.81 ± 0.03 in adult mice to 0.43 ± 0.04 in the aged *rdcl* group ($P < 0.0001$). However, despite an apparently greater iPLR response in the aged *rdcl* mice compared to aged *rd* mice, the variance in the iPLR responses was such that we could not detect a statistically significant difference between these two groups at any time point. There was also no significant difference between the iPLR of adult *rd* and adult *rdcl* mice.

Interestingly, there was also a significant effect of age by a two way ANOVA when comparing the congenic adult (7–9 months old) and aged (23 months old) C3H/He wild-type mice $P < 0.05$ ($F_{1,364} = 5.695$) (Fig. 4C). However, this was in the opposite direction, with aged wild types having a significantly reduced peak constriction compared to adult mice (0.42 ± 0.04 and 0.31 ± 0.03 respectively, $P < 0.05$). Representative iPLR recordings made from the isolated eyes of adult *rd* mice, aged *rd* mice and adult C3H/He wildtype, mice are shown respectively in Supplemental videos SV1, SV2 and SV3.

As shown in Fig. 4D, like the case in wild-type mice (Fig. 2A), the enhanced response in aged *rd* mice was also mediated to some extent by cholinergic transmission as atropine significantly slowed the time to peak constriction ($P < 0.001$) and sustained the constriction phase of the response. This was also the case for the smaller response found in younger *rd* mice ($n = 7$ eyes per group ± atropine, data not shown).

Baseline pupil tone increases in aged retinal degenerates

When conducting the iPLR recordings for the retinal degenerate mice, we noticed that the baseline (pre-stimulation) pupil tone appeared less in aged animals (compare adult and aged images in Fig. 4). To substantiate this observation we analyzed the baseline pupil area of mice from the various experimental groups. This analysis revealed a significant effect of experimental group (1-way ANOVA, $P < 0.0001$). As shown in Fig. 5A, B, post hoc analysis of the data confirmed that the pupils of aged *rd* mice were significantly smaller than those of adult *rd* mice ($P < 0.01$). The baseline pupils of adult *rd* animals were significantly more dilated than those of congenic adult wild types ($P < 0.01$) and the aged *rd* mice had comparable pupil tone to that of adult wild types (no significant difference detected). The baseline pupil areas of adult and aged *rdcl* mice were indistinguishable from those of the *rd* mice (data not shown).

As shown in Fig. 5, the application of atropine also increased baseline pupil area in both wild-type and aged *rd* eyes (Fig. 5A, B). Rather interestingly, we could find no difference between the baseline pupil area in adult wild-type and adult *Opn4*$^{-/-}$ mice, but a significant
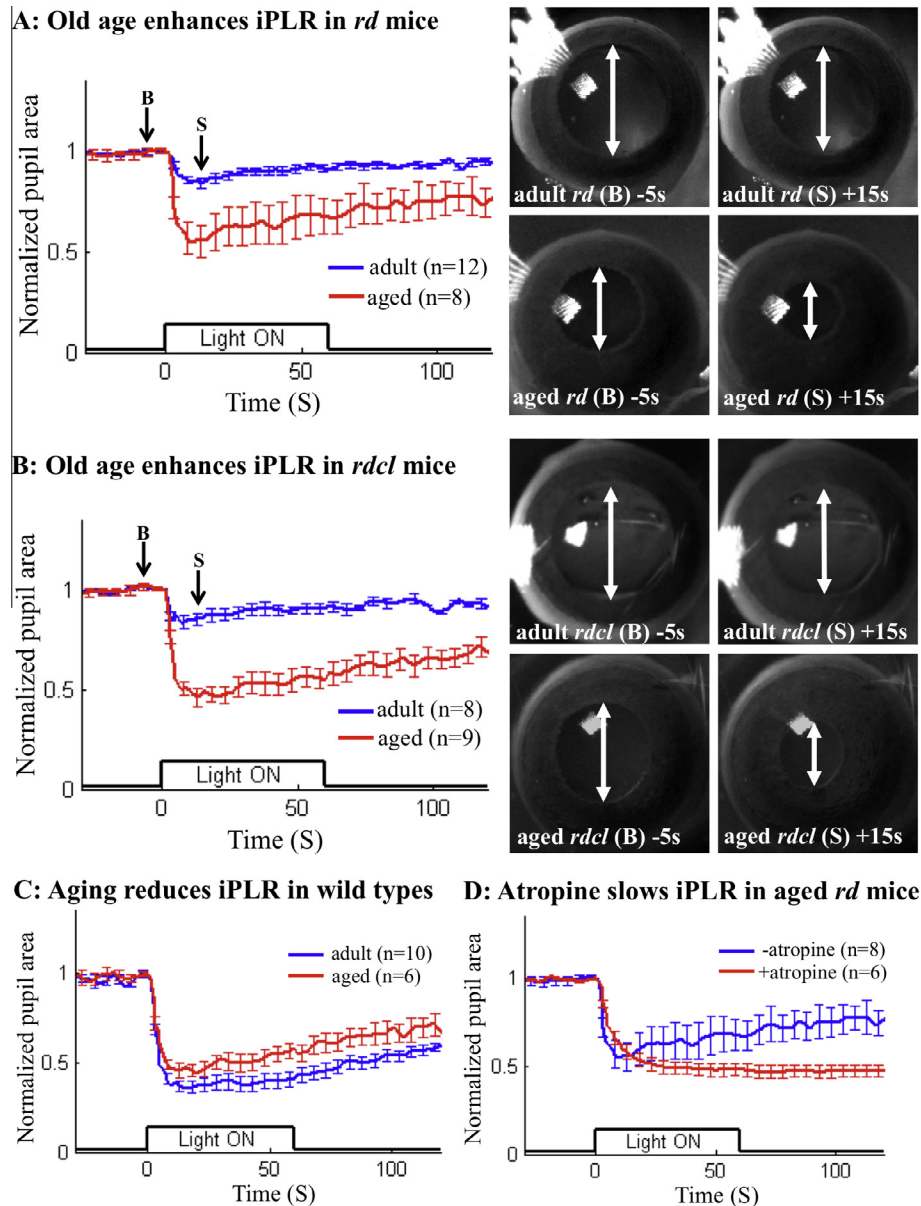
Fig. 4. Normal iPLR development requires an intact outer retina. The iPLR was dramatically reduced in both adult *rd* (A) and *rdcl* (B) mice compared to congenic C3H/He wild-type controls (C). Paradoxically, this response increases in aged *rd* (A) and *rdcl* (B) mice but decreases in aged wild types (C). Representative video stills are shown to the right where baseline (B) and stimulated (S) correspond to arrows on the associated graph. See also Supplemental videos SV1–3. (D) How atropine delays and prolongs the iPLR constriction in aged *rd* mice. Data points are the mean ± SEM and "*n*" = total number of eyes examined. Eyes were dark-adapted prior to stimulation with 60 s of white light at an irradiance of 63 mW/cm^2. For clarity, double-headed arrows indicate the relative size of each pupil.

reduction of baseline pupil tone (i.e. larger pupil diameter) in the triple knockout mice.

Together with the data in Fig. 4, our analysis shows that in mice with early and severe outer retinal degeneration both the baseline pupil tone and iPLR response fail to develop properly. Together with these observations, our baseline pupil data for adult wild-type, *Opn4$^{-/-}$* and *Opn4$^{-/-}$*, *Gnat1$^{-/-}$*, *Cnga3$^{-/-}$* (triple knockout) mice strongly suggest a role for the outer retina in generation of baseline pupil tone. However, there is also a paradoxical increase in the iPLR response in aged retinal degenerates, which is accompanied by an increase in baseline pupil tone in the absence of outer retina.

Melanopsin expression in iris and ciliary body of retinal degenerate mice

Previous work has shown that melanopsin is expressed in both the iris (Xue et al., 2011) and ciliary body (Semo et al., 2014) of mice. Given the results in the section 'Baseline pupil tone increases in aged retinal degenerates', we hypothesized that any increase in iPLR in aged *rd* mice may be due to increased melanopsin expression in the iris and/or ciliary body. To address this issue, we performed LCMD and quantitative real-time PCR on tissue from adult and aged *rd* mice as described in the section 'Laser capture microdissection (LCMD) and quantitative real-time PCR'. As shown in Fig. 6A, we
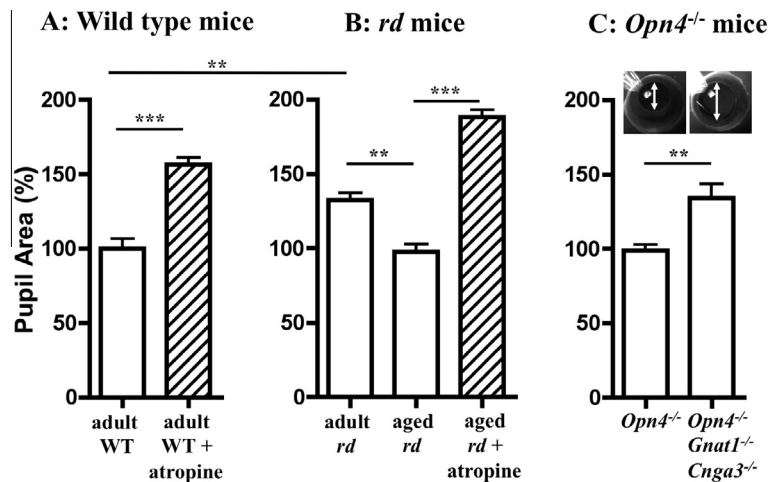
Fig. 5. Baseline (pre-stimulation) pupil tone is influenced by atropine and outer retinal degeneration. As shown in (A), the baseline pupil area of wild-type (WT) mice was significantly increased by atropine. Comparison with (B) shows how the baseline pupil area of adult *rd* mice was significantly elevated compared to that of adult WT and aged *rd* mice. Atropine also reduced baseline pupil tone in aged *rd* mice (B). While the baseline tone was indistinguishable in adult WT and $Opn4^{-/-}$ mice, the additional loss of outer retinal function in triple knockouts ($Opn4^{-/-}$, $Gnat1^{-/-}$, $Cnga3^{-/-}$) significantly decreased baseline pupil tone as reflected by increased pupil area (C). Pupil areas are expressed relative to the wild type (100%). Significance levels: $^{***}P < 0.001$, $^{**}P < 0.01$. For clarity, double-headed arrows indicate the relative size of each pupil.

found that both the iris and ciliary body of aged *rd* animals expressed less melanopsin than the same structures in adult *rd* mice. In particular, the level of gene expression in the ciliary body of aged *rd* samples was 50% less than that in the same structure of adult mice. The expression of the internal control gene (TBP) was detected in all samples and used to normalize values.

In addition to melanopsin, we also examined gene expression levels of rhodopsin in this tissue. This transcript was expressed at a very low level in all the samples but we were unable to reliably detect expression in all technical replicates (Fig. 6B). As we found the highest levels of rhodopsin expression in a single technical replicate of the iris of aged wild-type mice we cannot ascribe a great deal of confidence to this result. Interestingly, we were unable to detect rhodopsin transcript in the iris of *rd* mice. The latter finding was unexpected but entirely reproducible between technical replicates.

Immunohistochemistry for melanopsin in retinal degenerate mice

The retina of wild-type C3H/He mice has recently been shown to contain melanopsin-positive, Brn3b-negative cells that form a discrete plexus in the CMZ, which is most intense nasally (Semo et al., 2014). Following immunohistochemical staining for melanopsin, we were able to observe the same structure in adult *rdcl* mice (Fig. 7A). As shown in Fig. 7, this structure was most intense in the nasal hemiretina and there were numerous retino-ciliary projections clearly visible (arrows in Fig. 7B–E). Note also the bias toward superior and temporal regions in terms of ipRGC distribution (Fig. 7A).

Quantification and topography of RGCs in retinal degenerate mice. Using melanopsin immunohistochemistry to label ipRGCs, we analyzed the total ipRGC population

in 1–2-year-old C3H/He wild-type and *rdcl* mice. This analysis revealed a significant effect of retinal degeneration $P < 0.05$ ($F_{1,25} = 6.256$) and age $P < 0.01$ ($F_{2,25} = 7.308$) by a 2-way ANOVA and a significant reduction in ipRGCs at 1.5 years in the *rdcl* group by post hoc tests (Fig. 8A). This loss of ipRGCs was slower in wild-type mice but became more apparent in these animals at 2.5 years old, with a significant effect of age detectable in wild types from 1 to 2.5 years by a one-way ANOVA (data not shown).

In addition to the earlier loss of ipRGCs in *rdcl* mice, we could also detect a more generalized loss of RGCs in these animals as measured by the total number of Brn3a-positive cells (Fig. 8B). There was a significant effect of retinal degeneration $P < 0.001$ ($F_{1,18} = 17.81$), age $P < 0.05$ ($F_{1,18} = 5.53$) and an interaction between these two factors $P < 0.01$ ($F_{1,18} = 13.99$) by a 2-way ANOVA, with post hoc significance at 2 years ($P < 0.001$). The images in Fig. 8C–f also illustrate the reduction of ipRGCs and non-ipRGCs at 2 years of age.

In terms of spatial distribution, the k-nearest neighbor analysis revealed that the highest density of ipRGCs was to be found in superior and temporal regions of the retina in both C3H/He wild-type and *rdcl* mice at 1-year old and the superior retina at 2 years (Fig. 9). As shown in Fig. 9, the topography of Brn3a-positive RGCs also changed noticeably with age in the *rdcl* mice, with clear examples of sectoral loss in the inferior retina of these mice at 2 years of age.

Unfortunately, the retinal CMZ was not always present in retinas from aged animals due to technical difficulties with dissection. Therefore we were not able to compare this structure between adult and aged *rdcl* mice. However, when the melanopsin-positive CMZ plexus was visible in specimens from aged *rdcl* mice it appeared less obvious than the same structure in adult mice.
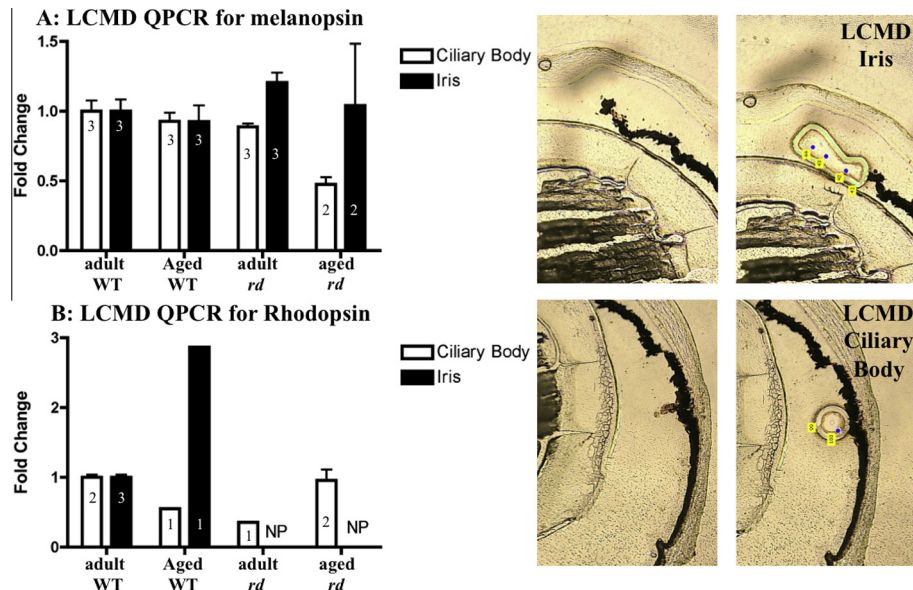
Fig. 6. Laser capture microdissection (LCMD) and quantitative real-time PCR (QPCR) for opsins in the iris and ciliary body of C3H/He wild-type (WT) and *rd* mice. The expression of melanopsin was not elevated in either structure of aged *rd* compared to adult *rd* mice (A). Rhodopsin expression was highest in the aged WT samples and not present (NP) in the iris of *rd* mice (B). Values are mean fold change ± SEM from *n* = 8 pooled samples in each group with *n* = 3 technical repeats per group normalized to TATA binding protein. Inset numbers on the chart indicate the number of technical replicates that resulted in amplification of product. Photomicrographs show representative images before (left) and after (right) LCMD of iris and ciliary body.
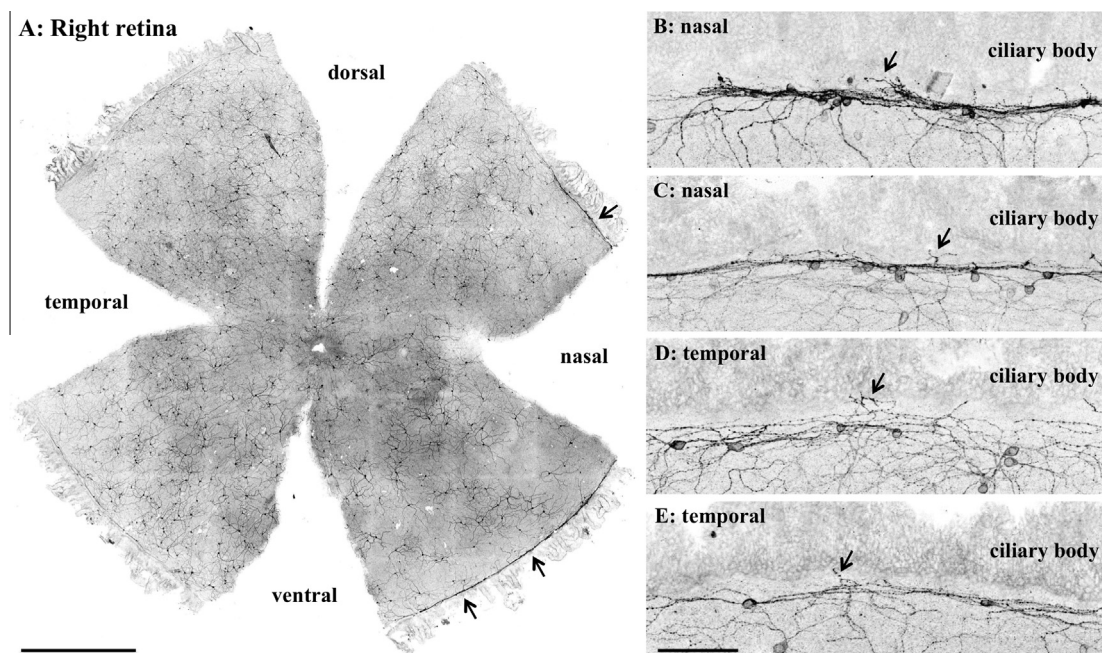

Fig. 7. Retinal degenerate mice retain a melanopsin-rich plexus in the retinal CMZ. The photomontage in (A) shows the entire right retina from an 8-month-old *rdcl* mouse. Images in (B–E) show higher magnification of the CMZ plexus in two nasal (A, C) and two temporal (D, E) regions. Arrows in A point to the nasal plexus while arrows in (B–E) point to examples of melanopsin-positive retino-ciliary projections. Scale bars: A = 1 mm, B–E = 100 µm.

Investigating a role for cones and rods in the generation of iPLR in mice

Given our finding that mice lacking outer retinal photoreceptors have a significantly reduced iPLR, we next sought to determine if preferential stimulation of the

outer retina with red light in *Opn1mw*[R] mice could drive the iPLR. This seemed particularly important given the distinct possibility of a direct pathway from retina into ciliary body/iris (Semo et al., 2014; Schmidt et al., 2014a).

As shown in Fig. 10A, our comparison between the influence of intense red light on pupil constriction in
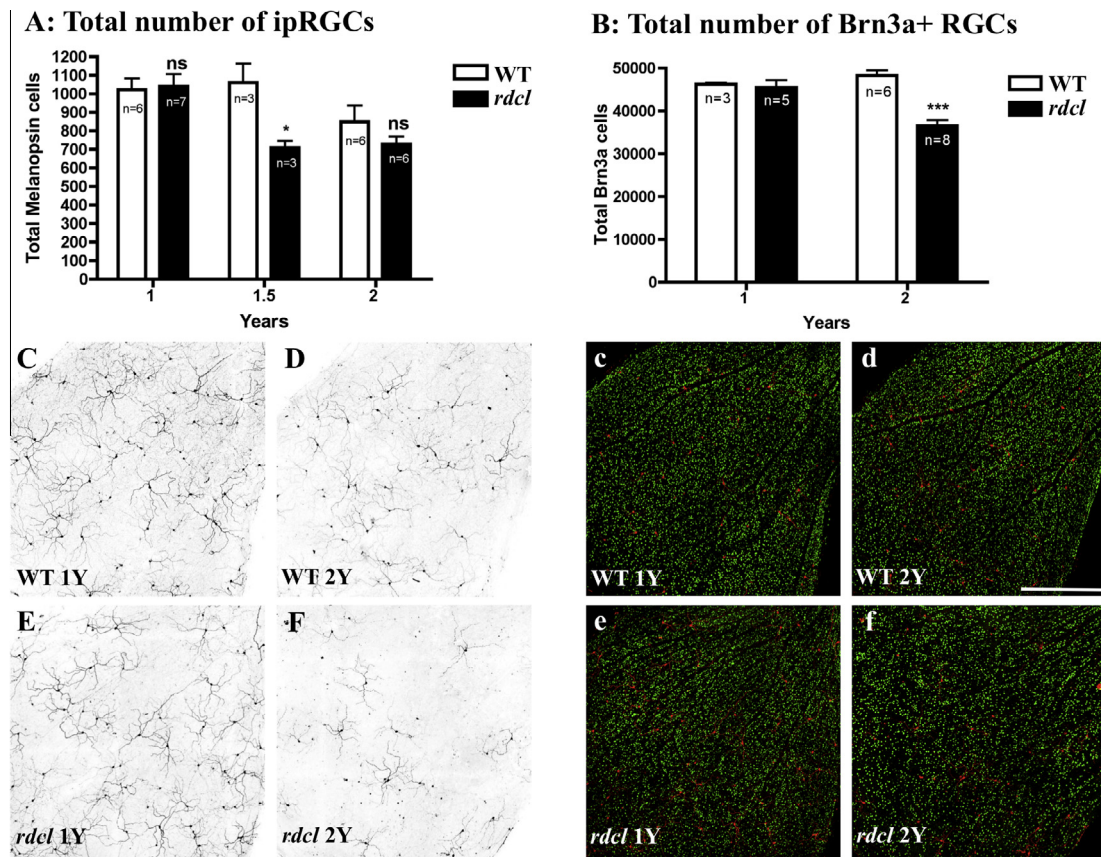
Fig. 8. Immunostaining for melanopsin and Brn3a reveal a preferential decline in ipRGCs and non-ipRGCs in aged *rdcl* mice. (A) ipRGCs decline earlier in *rdcl* mice than C3H/He wild types (WT). There is also a decline in non-ipRGC numbers at 2 years as assessed by Brn3a (B). The representative confocal images in (C–F) are taken from inferior nasal retina and illustrate how melanopsin immunoreactivity is reduced in aged mice. Brn3a was also stained on these retinae and both green (Brn3a) and red (melanopsin) channels are shown together in the corresponding merged images to the right (c–f). Significance levels: $^{*}P < 0.05$, $^{***}P < 0.001$. Scale bar = 500 μm. (For interpretation of the references to color in this figure legend, the reader is referred to the web version of this article.)

Opn1mw^R and wild-type C57BL/6 mice revealed no obvious difference between the groups, with an equally slow response to illumination in both. Analysis by a two-way ANOVA revealed no significant effect of genotype but a significant effect of time ($P < 0.0001$) ($F_{26,286} = 7.994$). There was no interaction between time and genotype and no significant differences found between *Opn1mw^R* and wild-type mice by Bonferroni post hoc analysis. Therefore, given that the action spectrum for melanopsin extends beyond 625 nm in mice (Lall et al., 2010), the slow constriction seen in both groups in Fig. 10A most likely reflects a small degree of melanopsin activation by the intense red light stimulus.

We next examined the iPLR in mice lacking either functional cones or functional rods to see if either pathology influenced the iPLR in adult mice. The Cone photoreceptor function loss 5 (*Cpfl5*) mouse is a naturally occurring model of achromatopsia with a missense mutation in exon 5 of the *Cnga3* gene that renders cone cyclic nucleotide-gated channels non-functional. These mice lack cone function (by photopic ERG) and exhibit a slow degeneration of cones (Pang et al., 2012). As shown in Fig. 10B, we observed a robust iPLR in these animals indicating that cone function is not essential for the development of iPLR in mice. The

Gnat1$^{-/-}$ (rod alpha transducin knockout) mouse is a model of congenital stationary night blindness exhibiting an absence of rod function (by scotopic ERG) and a slow degeneration of rods (Calvert et al., 2000; Pearson et al., 2012). As shown in Fig. 10C, this mutation appeared to dramatically reduce the iPLR, with *Gnat1$^{-/-}$* mice exhibiting a small and transient constriction in response to light.

The iPLR fails to develop properly in hypo-pigmented mice

Due to the mixed strain background of the *Cpfl5* mice, littermates of the same genotype sometimes vary in coat color, being either agouti or black. We noticed while recording iPLRs from these mice that the response appeared weaker in agouti animals. This is illustrated by the separation of the *Cpfl5* data into agouti and black groups (Fig. 10B). We found that there was indeed a significant effect of coat color by a 2-way ANOVA ($P < 0.001$, $F_{1,264} = 11.19$), with peak constrictions of 0.50 ± 0.04 and 0.32 ± 0.05 for agouti and black-coated mice respectively (*t*-test, $P = 0.01$).

The *Gnat1$^{-/-}$* mice used here were a light caramel color, a phenotype resulting from the mixture 129/Sv and BALB/c used to generate founder mice (Calvert
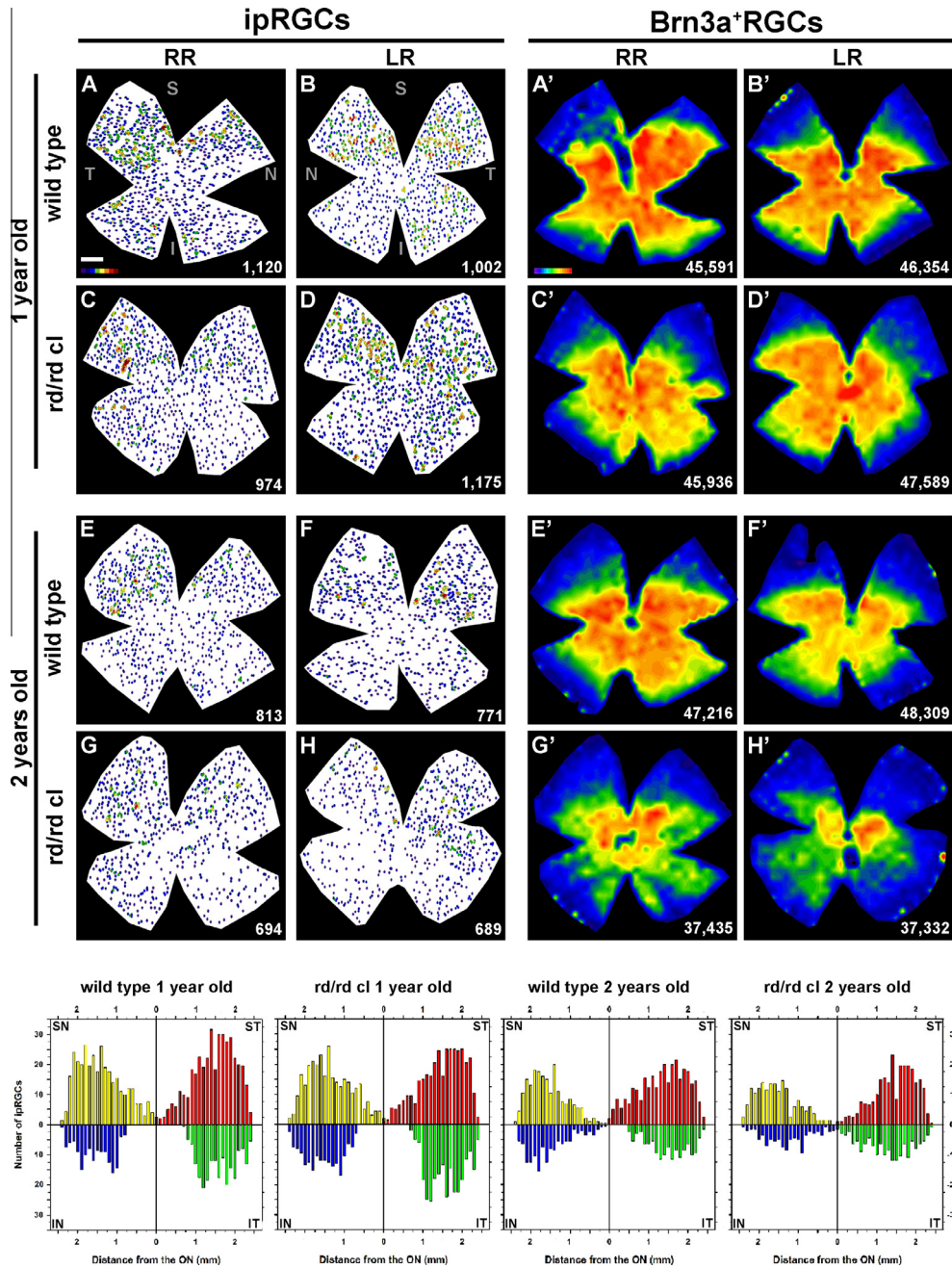
Fig. 9. Examples showing the spatial distribution of ipRGCs (stained for melanopsin) and non-ipRGCs (stained for Brn3a) in C3H/He wildtype and *rdcl* mice of 1 and 2 years. Total cells counted are shown bottom right of each whole mount image. All images are color coded to show cell density. For the k-nearest neighbor plots (A–D and E–H) this scale ranges from 0 neighbors (purple) to > 11 neighbors (red) within a 200-μm radius. For the Brn3a + RGC plots (A'–D' and E'–H') purple indicates 0 RGCs/mm² and red > 4800 RGCs/mm². Quadrant analysis of the neighbor data from 4 retinas is shown at the bottom, where ipRGC number is plotted against distance from the ON in mm. *Abbreviations:* Right retina (RR), left retina (LR), optic nerve (ON) and ' denotes paired plots from the same retina. (For interpretation of the references to color in this figure legend, the reader is referred to the web version of this article.)

et al., 2000). In order to examine if pigmentation could have influenced the results in *Gnat1⁻/⁻* mice we measured the iPLR in age-matched BALB/c mice, which are albino. As shown in Fig. 10D, the BALB/c gave a very similar iPLR response to *Gnat1⁻/⁻* mice, with a small, transient response and an inability to sustain constriction. To provide further evidence that pigmentation is required for iPLR development we also examined this response in

albino MF1 mice (Fig. 10E). Again, the iPLR in these mice was small and reminiscent of that seen in adult *rd* and *rdcl* mice (compare Fig. 10E with Fig. 4A, B).

DISCUSSION

Here we validate a new *in vitro* technique for studying the iPLR in mice. This technique has a distinct advantage
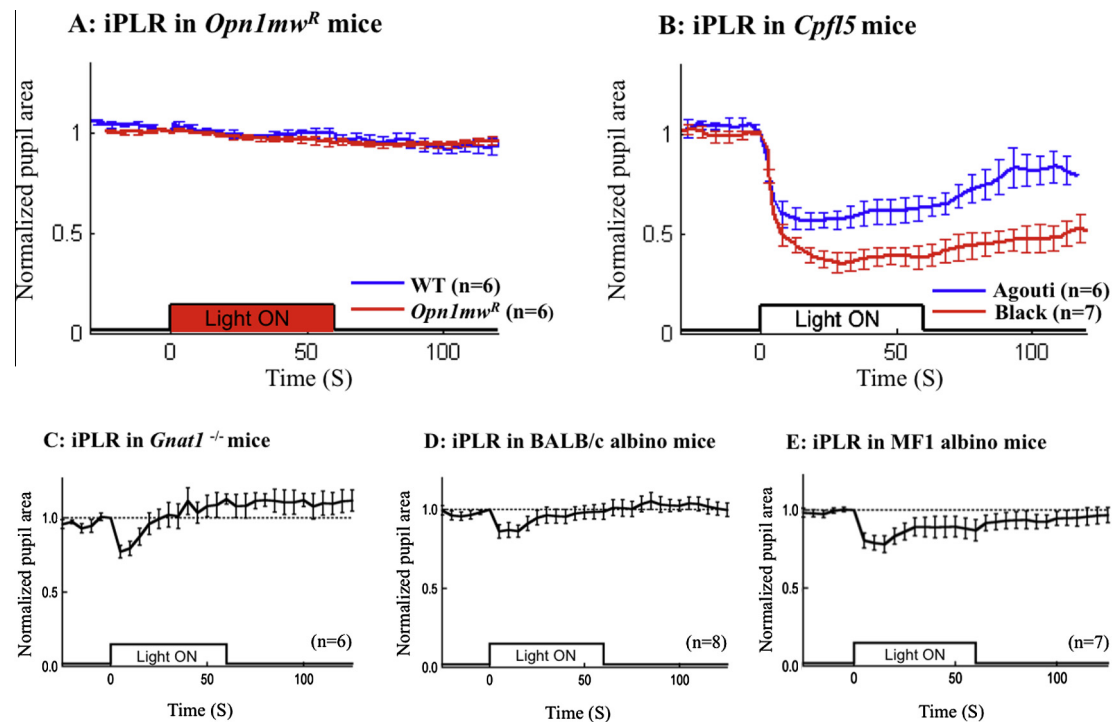
Fig. 10. The iPLR is unaffected by preferential retinal stimulation and loss of cone function but loss of rod function and/or pigmentation appear essential for normal iPLR development in mice. As shown in (A), using 60 s of red light (625–650 nm $\sim 1.2 \times 10^{16}$ photons/cm^2/s) to preferentially stimulate cones in *Opn1mw^R* mice, we found no difference between the iPLR in *Opn1mw^R* and C57BL/6 wild-type (WT) controls, with pupil tone increasing significantly over time equally for both groups. A robust iPLR was present in cone photoreceptor function loss 5 (*Cpfl5*) mice (B) but not the rod-function deficient *Gnat1$^{-/-}$* mice (C). However, analysis of pigmentation phenotype revealed that the iPLR was significantly reduced in agouti verses black mice (B) and severely degraded in albino mice of the BALB/c (D) and MF1 (E) strains. In (B–E), eyes were dark-adapted prior to stimulation with 60 s of white light at an irradiance of 63 mW/cm^2.

over existing *in vitro* methods (Bito and Turansky, 1975; Tu et al., 2004; Xue et al., 2011) in that it allows any contribution from the ciliary body/retina to also be measured without the necessity to perform difficult axotomy surgery in living animals. In addition to confirming a role for melanopsin and cholinergic signaling in the iPLR, our validation experiments also revealed new properties of this response in mice. Namely, we found that the iPLR occurs readily under light-adapted conditions and that surprisingly brief pulses of light ($\geqslant 50$ ms) can elicit it. This stimulus duration experiment was particularly important for showing that the sustained response and slow recovery we observe after 60 s of light stimulation is unlikely to be due to saturation of the iPLR system by constant light exposure.

This is the first description of the time course of iPLR development in mice, with an absence of responsiveness at P17 and a slow postnatal maturation between P21 and P49 in wild-type animals. This was surprising given that in mice, the melanopsin system is functional from birth (Sekaran et al., 2005) and the conventional PLR is first detected at P7, developing to adult levels by P10 (McNeill et al., 2011). In C57BL/6 mice, there is a progressive development of synaptic connectivity in the retina between P12 and adulthood (Sherry et al., 2003), together with a slow maturation of retinal function (as measured by ERG) between eye opening at $\sim$P14 and

P28 (Takada et al., 2004). Consequently, in contrast to the conventional PLR which arises in the absence of outer retinal signaling (McNeill et al., 2011), it may be that the iPLR requires retinal activity to mature properly.

The late emergence of iPLR in mice may also reflect a delay in the innervation of the ciliary body / iris by the axons from melanopsin-positive retinal neurons. This would be similar to the late maturation of the M1 ipRGC projection to the suprachiasmatic nucleus in mice which continues until $\sim$P21 (McNeill et al., 2011). As the melanopsin-positive cells of the mouse CMZ are M1-like and mainly negative for Brn3b (Semo et al., 2014) they may also be members of the discrete population of Brn3b-negative ipRGCs which drive circadian responses in mice (Chen et al., 2011).

More direct evidence for a role of outer retina in the development of iPLR comes from our findings of a reduced iPLR response in adult mice lacking rods (*rd*) or rods and cones (*rdcl*). As both mice carry the *rd* mutation in the beta subunit of cGMP-specific phospodiesterase we were keen to rule out a general effect of this mutation on the iPLR. As such, we attempted to block the iPLR in wild-type mice using the cGMP-PDE inhibitor Zaprinast (100 μM and 1 mM, data not shown), which had no effect. Unlike wildtype mice, the small iPLR response in adult rd mice was also detectable at P17 suggesting that melanopsin in the iris

sphincter muscle is functional from an early stage in these animals. It is difficult to reconcile this with the absence of constriction in P17 wild types at this stage but the difference may reflect another role for outer retina in regulating iridial constriction during early development.

The *rd* mutation renders all rods in *rd* and *rdcl* non-functional from birth. In addition to this, the *rdcl* mice also have a diphtheria-targeted destruction of cones at the onset of cone opsin expression (Soucy et al., 1998). So, although both strains will lack rods by the end of the third postnatal week, the *rd* mice will retain some cone function until adult life (Strettoi et al., 2002; Thyagarajan et al., 2010). This limited cone function was not sufficient to cause a statistically significant difference between the iPLR in *rd* and *rdcl* mice. Taken together with the robust response observed in the *Cpfl5* animals and a lack of cone-driven constriction in adult *Opn1mw^R* mice it would appear that cones play no role in the development of iPLR in mice. In fact, it would appear from the results in *rd* and *Gnat1$^{-/-}$* mice that rods exert the major outer retinal influence on iPLR development (although, see discussion below pertaining to the hypopigmentation in *Gnat1$^{-/-}$* mice). However, this does not agree with the findings of Xue and colleagues who could find no deficit in the constriction of iris sphincter muscles isolated from rhodopsin knockout mice (Xue et al., 2011).

Given that the amplitude of the conventional PLR remains stable with advancing age in *rdcl* mice (Semo et al., 2003b), we were absolutely amazed to find an almost wild-type level of iPLR response and baseline pupil tone in the aged retinal degenerate mice. At the present time we find this difference somewhat difficult to explain. Our immediate thought was that perhaps melanopsin expression had increased in a compensatory fashion in the iris of aged retinal degenerates but we could find no evidence for this. Neither could we detect any obvious deficit in the nasal melanopsin plexus of adult retinal degenerates, with clear examples of melanopsin-positive processes extending into the ciliary body of the animals (see Fig. 7). Due to technical difficulties, we were not able to compare the CMZ between adult and aging *rdcl* mice but it remains possible that any retinal melanopsin neurons projecting to the iris may be reacting positively to advancing age in these mice.

Our quantification of ipRGCs revealed an age-dependent loss of melanopsin-positive cells in both wild-types and *rdcl* at advanced age (over 2 years of age). This is in agreement with an earlier ipRGC sampling study (Semo et al., 2003a) and a demonstrated reduction in retinal afferents to the suprachiasmatic nucleus in aged wild types and *rdcl* (Lupi et al., 2012). However, here we extend on these findings showing that the loss of melanopsin-positive cells is accelerated in *rdcl* mice, occurring earlier than the wildtypes at 1.5 years of age. This finding most likely reflects the preferential loss of RGCs we report in aged *rdcl* mice (Fig. 8B) and also agrees with RGC loss in aging *rd* mice (Wang et al., 2000) and a loss of ipRGCs with increasing age in rat models of retinitis pigmentosa (Vugler et al., 2008; Esquiva et al., 2013). Interestingly, the topography of ipRGCs in 1-year-old C3H/He wild-type and *rdcl* retinas showed a bias toward superior and tem-

poral regions which agrees with a recent report in C57BL/6 mice (Valente-Soriano et al., 2014).

The increase in iPLR amplitude in aging retinal degenerate mice was accompanied by an increase in the baseline pupil tone in these animals to a level that was indistinguishable from adult wild-type mice. Atropine application significantly increased baseline pupil area in both adult wild-type and aged *rd* mice suggesting that in both cases, the maintenance of dark-adapted pupil tone requires cholinergic neurotransmission. This may simply reflect a blockade of autonomic cholinergic signaling between ciliary nerve and iris muscles but could also involve a retinal mechanism as topical atropine application readily alters retinal function in mice (Semo et al., 2010).

Rather interestingly, the pupil tone in adult *OPN4$^{-/-}$* mice was similar to that in adult wild-type mice but significantly greater than that observed in adult triple knockout mice of the same strain. As the latter mice lack rod and cone function, this result, together with the reduced pupil tone in adult *rd* mice strongly suggests a role for the outer retina in either the development or generation of dark-adapted pupil tone in mice.

At this stage we can only speculate about the underlying mechanisms at play here but a reasonable explanation could involve an outer retinal-driven modulation of ipRGC activity in the dark. It is known that the resting trans-membrane voltage (V_m) of RGCs is regulated to some extent by the ON pathway (Margolis and Detwiler, 2007) and that in darkness, the V_m of ipRGCs can be changed by pharmacological manipulation of outer retinal signaling (Schmidt and Kofuji, 2010). So, it seems plausible that the reduction in baseline pupil tone in adult *rd* and triple knockout mice could result from a change in the dark-adapted tonic firing rate of any melanopsin neurons that project from the retina into the iris. Likewise, in the aged *rd* mice, there may have been some adaptation in the melanopsin neurons of the CMZ causing them to increase tonic activity in the dark. It would be interesting to test this hypothesis by measuring the V_m of ipRGCs in adult verses aged *rd* mice. An alternative explanation could involve a progressive reduction in tonic ipRGC drive to the iris muscles of *rd* mice as these cells are lost during advanced aging. Such a scenario could result in proportionately more sphincter-generated force and smaller baseline pupils.

Our results with atropine suggest that if the outer retina (via ipRGCs) does indeed regulate baseline pupil tone, this is likely to be mediated by cholinergic neurotransmission either at the level of retinal amacrine cells or within the iris itself. In terms of the melanopsin neurons performing any retinal-iridial signaling, we speculate that they may use pituitary adenylate cyclase-activating polypeptide (PACAP), which most likely underlies the slower conventional PLR responses obtained from mice whose ipRGCs lack vesicular glutamate transporter 2 (Delwig et al., 2013). Given that PACAP receptor 1 knockout mice show an attenuation of the sustained phase of the PLR at high irradiance, it would be interesting to examine the iPLR in these animals using our new method.

In addition to a new role for the outer retina, we also found a strong influence of pigmentation on the development of iPLR in mice. We found a significant effect of coat color on the iPLR in *Cpfl5* mice and a small and transient response in two strains of albino mice. One of these strains was the BALB/c, which was used to generate the $Gnat1^{-/-}$ line (Calvert et al., 2000) also studied here. Based on our results, we suspect that the small, transient iPLR in $Gnat1^{-/-}$ mice is mainly caused by the hypopigmentation generated as a result of their mixed BALB/c background. However, as we did not have access to the congenic controls for these mice, we were not able to rule out a role for the rod mutation in these experiments.

Our findings in albino mice are consistent with previous work which failed to detect a significant intrinsic pupil response in axotomized albino rats (Lau et al., 1992). However, they are not consistent with the results of Xue and colleagues who reported that the constriction of isolated albino mouse and albino rat sphincter muscles was actually stronger than the pigmented counterparts. This most likely reflects the fact that isolating the iris sphincter muscle will only allow visualization of that component of iPLR which involves the sphincter muscle. Given these results, it may be that there is some developmental abnormality in albino mice that prevents the retinal-driven component of this response, for instance, an inability of ipRGCs to relax the iris dilator muscle (Semo et al., 2014). In support of this idea, albino rodents have significantly more RGCs (Williams et al., 1996; Salinas-Navarro et al., 2009) together with deficits in axonal targeting (Lund, 1965), rod numbers (Donatien and Jeffery, 2002), cone topography (Ortin-Martinez et al., 2014) and displaced ipRGCs (Nadal-Nicolas et al., 2014; Valente-Soriano et al., 2014). It may well be therefore one or all of these factors contribute to the reduced iPLR we see in albino mice. Alternatively, because melanin has intense calcium-binding/buffering capacity (Balkema and Drager, 1990), it's absence in the albino iris/ciliary body may reduce sustained muscle contraction. It is particularly interesting that the number of rods appears to decline as a function of hypopigmentation in mice (Donatien and Jeffery, 2002), an observation that may help to explain our result in agouti mice. A loss of rods with aging (Gresh et al., 2003) may also help to explain the subtle decline in iPLR we observed in aged wild-type mice.

CONCLUSIONS

Here we describe a new *in vitro* technique for studying the iPLR. We show that this response develops unexpectedly late in mice, making it unlikely that a melanopsin-dependent iPLR would participate in driving neonatal light aversion in mice (Johnson et al., 2010). In addition to melanopsin, our results strongly implicate rods and ocular pigmentation in the development of the iPLR in mice. We report a paradoxical increase in the strength of iPLR with increasing age in *rd* and *rdcl* mice that reflects an increase in the potency of melanopsin signaling despite a decline in ipRGCs. This phenomenon may help to explain the age-dependent increase in behavioral light sensitivity we have reported previously in *rdcl* mice (Semo et al., 2010). Furthermore, because the *rd* mutation occurs in patients with retinitis pigmentosa, our findings may also be relevant to understanding the progression of sleep disturbances and photophobia and in these patients, who also experience increased sensitivity to light with progressive RGC loss (Hamel, 2006; Vugler, 2010).

Finally, recent experiments using genetic tools to ablate melanopsin-expressing cells in mice conclude that a subpopulation of ∼200 Brn3b-negative ipRGCs is sufficient to photoentrain circadian behavior (Guler et al., 2008; Chen et al., 2011). Given that the genetic ablation of melanopsin-expressing cells would also presumably include cells of the iris / ciliary body, it appears conceivable that pupillary constriction in mice could in someway contribute toward circadian photoentrainment independent of the brain, perhaps using some trigeminal-based signaling route (Noseda et al., 2010).

AUTHOR CONTRIBUTIONS

CG: iPLR study design, design and implementation of the iPLR analysis software, performed iPLR experiments, analysis and interpretation of iPLR data; AV: All study designs, performed iPLR experiments, data analysis and interpretation, microscopy, wrote the manuscript with contributions from CG, MS and MV-S; MS: Contributed to iPLR and anatomical study designs, designed performed and analyzed the LCMD-QPCR experiment, analysis of iPLR data, microscopy; A.O-M: Anatomical study design, immunohistochemistry, microscopy, analysis and interpretation of anatomical data; AR: Performed wild-type iPLR developmental experiment, data analysis and interpretation; BN: Performed the LCMD-QPCR experiment; FJVS: Analysis and interpretation of anatomical data; D.G-A: Analysis and interpretation of anatomical data; PC: contributed toward the adult aging component of iPLR and anatomical studies; MV-S: Anatomical study design, anatomical methodology and interpretation of anatomical data.

REFERENCES

Alexandridis E (1985) Die Pupille: Physiologie-Untersuchung-Pathologie. New York: Springer-Verlag.

Allen AE, Storchi R, Martial FP, Petersen RS, Montemurro MA, Brown TM, Lucas RJ (2014) Melanopsin-driven light adaptation in mouse vision. Curr Biol 24(21):1–10.

Asteriti S, Gargini C, Cangiano L (2014) Mouse rods signal through gap junctions with cones. eLife 3:e01386.

Balkema GW, Drager UC (1990) Origins of uncrossed retinofugal projections in normal and hypopigmented mice. Vis Neurosci 4:595–604.

Barr L, Alpern M (1963) Photosensitivity of the frog iris. J Gen Physiol 46:1249–1265.

Baver SB, Pickard GE, Sollars PJ, Pickard GE (2008) Two types of melanopsin retinal ganglion cell differentially innervate the hypothalamic suprachiasmatic nucleus and the olivary pretectal nucleus. Eur J Neurosci 27:1763–1770.

Bito LZ, Turansky DG (1975) Photoactivation of pupillary constriction in the isolated in vitro iris of a mammal (*Mesocricetus auratus*). Comp Biochem Physiol A Comp Physiol 50:407–413.

Brown TM, Gias C, Hatori M, Keding SR, Semo M, Coffey PJ, Gigg J, Piggins HD, Panda S, Lucas RJ (2010) Melanopsin contributions to irradiance coding in the thalamo-cortical visual system. PLoS Biol 8:e1000558.

Brown TM, Tsujimura S, Allen AE, Wynne J, Bedford R, Vickery G, Vugler A, Lucas RJ (2012) Melanopsin-based brightness discrimination in mice and humans. Curr Biol 22:1134–1141.

Calvert PD, Krasnoperova NV, Lyubarsky AL, Isayama T, Nicolo M, Kosaras B, Wong G, Gannon KS, Margolskee RF, Sidman RL, Pugh Jr EN, Makino CL, Lem J (2000) Phototransduction in transgenic mice after targeted deletion of the rod transducin alpha-subunit. Proc Natl Acad Sci U S A 97:13913–13918.

Chen SK, Badea TC, Hattar S (2011) Photoentrainment and pupillary light reflex are mediated by distinct populations of ipRGCs. Nature 476:92–95.

Dacey DM, Liao HW, Peterson BB, Robinson FR, Smith VC, Pokorny J, Yau KW, Gamlin PD (2005) Melanopsin-expressing ganglion cells in primate retina signal colour and irradiance and project to the LGN. Nature 433:749–754.

Delwig A, Majumdar S, Ahern K, LaVail MM, Edwards R, Hnasko TS, Copenhagen DR (2013) Glutamatergic neurotransmission from melanopsin retinal ganglion cells is required for neonatal photoaversion but not adult pupillary light reflex. PLoS One 8:e83974.

Donatien P, Jeffery G (2002) Correlation between rod photoreceptor numbers and levels of ocular pigmentation. Invest Ophthalmol Vis Sci 43:1198–1203.

Ecker JL, Dumitrescu ON, Wong KY, Alam NM, Chen SK, Legates T, Renna JM, Prusky GT, Berson DM, Hattar S (2010) Melanopsin-expressing retinal ganglion-cell photoreceptors: cellular diversity and role in pattern vision. Neuron 67:49–60.

Esquiva G, Lax P, Cuenca N (2013) Impairment of intrinsically photosensitive retinal ganglion cells associated with late stages of retinal degeneration. Invest Ophthalmol Vis Sci 54:4605–4618.

Estevez ME, Fogerson PM, Ilardi MC, Borghuis BG, Chan E, Weng S, Auferkorte ON, Demb JB, Berson DM (2012) Form and function of the M4 cell, an intrinsically photosensitive retinal ganglion cell type contributing to geniculocortical vision. J Neurosci 32:13608–13620.

Fan J, Rohrer B, Moiseyev G, Ma JX, Crouch RK (2003) Isorhodopsin rather than rhodopsin mediates rod function in RPE65 knock-out mice. Proc Natl Acad Sci U S A 100:13662–13667.

Galindo-Romero C, Jimenez-Lopez M, Garcia-Ayuso D, Salinas-Navarro M, Nadal-Nicolas FM, Agudo-Barriuso M, Villegas-Perez MP, Aviles-Trigueros M, Vidal-Sanz M (2013) Number and spatial distribution of intrinsically photosensitive retinal ganglion cells in the adult albino rat. Exp Eye Res 108:84–93.

Ghosh S, Salvador-Silva M, Coca-Prados M (2004) The bovine iris-ciliary epithelium expresses components of rod phototransduction. Neurosci Lett 370:7–12.

Gresh J, Goletz PW, Crouch RK, Rohrer B (2003) Structure–function analysis of rods and cones in juvenile, adult, and aged C57bl/6 and Balb/c mice. Vis Neurosci 20:211–220.

Guler AD, Ecker JL, Lall GS, Haq S, Altimus CM, Liao HW, Barnard AR, Cahill H, Badea TC, Zhao H, Hankins MW, Berson DM, Lucas RJ, Yau KW, Hattar S (2008) Melanopsin cells are the principal conduits for rod-cone input to non-image-forming vision. Nature 453:102–105.

Hamel C (2006) Retinitis pigmentosa. Orphanet J Rare Dis 1:40.

Hannibal J, Hindersson P, Knudsen SM, Georg B, Fahrenkrug J (2002) The photopigment melanopsin is exclusively present in pituitary adenylate cyclase-activating polypeptide-containing retinal ganglion cells of the retinohypothalamic tract. J Neurosci 22:RC191.

Hattar S, Kumar M, Park A, Tong P, Tung J, Yau KW, Berson DM (2006) Central projections of melanopsin-expressing retinal ganglion cells in the mouse. J Comp Neurol 497:326–349.

Hattar S, Liao HW, Takao M, Berson DM, Yau KW (2002) Melanopsin-containing retinal ganglion cells: architecture, projections, and intrinsic photosensitivity. Science 295:1065–1070.

Hattar S, Lucas RJ, Mrosovsky N, Thompson S, Douglas RH, Hankins MW, Lem J, Biel M, Hofmann F, Foster RG, Yau KW (2003) Melanopsin and rod-cone photoreceptive systems account for all major accessory visual functions in mice. Nature 424:76–81.

Hughes S, Watson TS, Foster RG, Peirson SN, Hankins MW (2013) Nonuniform distribution and spectral tuning of photosensitive retinal ganglion cells of the mouse retina. Curr Biol 23:1696–1701.

Johnson J, Wu V, Donovan M, Majumdar S, Renteria RC, Porco T, Van Gelder RN, Copenhagen DR (2010) Melanopsin-dependent light avoidance in neonatal mice. Proc Natl Acad Sci U S A 107:17374–17378.

Joo HR, Peterson BB, Dacey DM, Hattar S, Chen SK (2013) Recurrent axon collaterals of intrinsically photosensitive retinal ganglion cells. Vis Neurosci 30:175–182.

Lall GS, Revell VL, Momiji H, Al Enezi J, Altimus CM, Guler AD, Aguilar C, Cameron MA, Allender S, Hankins MW, Lucas RJ (2010) Distinct contributions of rod, cone, and melanopsin photoreceptors to encoding irradiance. Neuron 66:417–428.

Lau KC, So KF, Campbell G, Lieberman AR (1992) Pupillary constriction in response to light in rodents, which does not depend on central neural pathways. J Neurol Sci 113:70–79.

Lucas RJ, Hattar S, Takao M, Berson DM, Foster RG, Yau KW (2003) Diminished pupillary light reflex at high irradiances in melanopsin-knockout mice. Science 299:245–247.

Lund RD (1965) Uncrossed visual pathways of hooded and albino rats. Science 149:1506–1507.

Lupi D, Semo M, Foster RG (2012) Impact of age and retinal degeneration on the light input to circadian brain structures. Neurobiol Aging 33:383–392.

Margolis DJ, Detwiler PB (2007) Different mechanisms generate maintained activity in ON and OFF retinal ganglion cells. J Neurosci 27:5994–6005.

McNeill DS, Sheely CJ, Ecker JL, Badea TC, Morhardt D, Guido W, Hattar S (2011) Development of melanopsin-based irradiance detecting circuitry. Neural Dev 6:8.

Nadal-Nicolas F, Salinas-Navarro M, Jimenez-Lopez M, Sobrado-Calvo P, Villegas-Pérez MP, Vidal-Sanz M, Agudo-Barriuso M (2014) Displaced retinal ganglion cells in albino and pigmented rats. Front Neuroanat 8:1–21.

Nadal-Nicolas FM, Jimenez-Lopez M, Sobrado-Calvo P, Nieto-Lopez L, Canovas-Martinez I, Salinas-Navarro M, Vidal-Sanz M, Agudo M (2009) Brn3a as a marker of retinal ganglion cells: qualitative and quantitative time course studies in naive and optic nerve-injured retinas. Invest Ophthalmol Vis Sci 50:3860–3868.

Noseda R, Kainz V, Jakubowski M, Gooley JJ, Saper CB, Digre K, Burstein R (2010) A neural mechanism for exacerbation of headache by light. Nat Neurosci 13:239–245.

Ortin-Martinez A, Nadal-Nicolas FM, Jimenez-Lopez M, Alburquerque-Bejar JJ, Nieto-Lopez L, Garcia-Ayuso D, Villegas-Perez MP, Vidal-Sanz M, Agudo-Barriuso M (2014) Number and distribution of mouse retinal cone photoreceptors: differences between an albino (Swiss) and a pigmented (C57/BL6) strain. PLoS One 9:e102392.

Panda S, Provencio I, Tu DC, Pires SS, Rollag MD, Castrucci AM, Pletcher MT, Sato TK, Wiltshire T, Andahazy M, Kay SA, Van Gelder RN, Hogenesch JB (2003) Melanopsin is required for non-image-forming photic responses in blind mice. Science 301:525–527.

Pang JJ, Deng WT, Dai X, Lei B, Everhart D, Umino Y, Li J, Zhang K, Mao S, Boye SL, Liu L, Chiodo VA, Liu X, Shi W, Tao Y, Chang B, Hauswirth WW (2012) AAV-mediated cone rescue in a naturally occurring mouse model of CNGA3-achromatopsia. PLoS One 7:e35250.

Pearson RA, Barber AC, Rizzi M, Hippert C, Xue T, West EL, Duran Y, Smith AJ, Chuang JZ, Azam SA, Luhmann UF, Benucci A, Sung CH, Bainbridge JW, Carandini M, Yau KW, Sowden JC, Ali RR (2012) Restoration of vision after transplantation of photoreceptors. Nature 485:99–103.

Peirson SN, Bovee-Geurts PH, Lupi D, Jeffery G, DeGrip WJ, Foster RG (2004) Expression of the candidate circadian photopigment melanopsin (Opn4) in the mouse retinal pigment epithelium. Brain Res Mol Brain Res 123:132–135.

Peirson SN, Butler JN, Foster RG (2003) Experimental validation of novel and conventional approaches to quantitative real-time PCR data analysis. Nucleic Acids Res 31:e73.

Pfaffl MW (2001) A new mathematical model for relative quantification in real-time RT-PCR. Nucleic Acids Res 29. E45-45.

Pires SS, Hughes S, Turton M, Melyan Z, Peirson SN, Zheng L, Kosmaoglou M, Bellingham J, Cheetham ME, Lucas RJ, Foster RG, Hankins MW, Halford S (2009) Differential expression of two distinct functional isoforms of melanopsin (Opn4) in the mammalian retina. J Neurosci 29:12332–12342.

Rupp A, Schmidt T, Chew K, Yungher B, Park K, Hattar S (2013) ipRGCs mediate ipsilateral pupil constriction. ARVO Annual Meeting Abstract 310.

Salinas-Navarro M, Jimenez-Lopez M, Valiente-Soriano FJ, Alarcon-Martinez L, Aviles-Trigueros M, Mayor S, Holmes T, Lund RD, Villegas-Perez MP, Vidal-Sanz M (2009) Retinal ganglion cell population in adult albino and pigmented mice: a computerized analysis of the entire population and its spatial distribution. Vision Res 49:637–647.

Schmidt T, Rupp A, Chew K, Yungher B, Cui Y, Wess J, Park K, Hattar S (2014a) A retinal projection to the iris mediates pupil constriction. ARVO Annual Meeting Abstract 1231.

Schmidt TM, Alam NM, Chen S, Kofuji P, Li W, Prusky GT, Hattar S (2014b) A role for melanopsin in alpha retinal ganglion cells and contrast detection. Neuron 82:781–788.

Schmidt TM, Kofuji P (2010) Differential cone pathway influence on intrinsically photosensitive retinal ganglion cell subtypes. J Neurosci 30:16262–16271.

Schmidt TM, Taniguchi K, Kofuji P (2008) Intrinsic and extrinsic light responses in melanopsin-expressing ganglion cells during mouse development. J Neurophysiol 100:371–384.

Sekaran S, Lupi D, Jones SL, Sheely CJ, Hattar S, Yau KW, Lucas RJ, Foster RG, Hankins MW (2005) Melanopsin-dependent photoreception provides earliest light detection in the mammalian retina. Curr Biol 15:1099–1107.

Seliger HH (1962) Direct action of light in naturally pigmented muscle fibers. I. Action spectrum for contraction in eel iris sphincter. J Gen Physiol 46:333–342.

Semo M, Gias C, Ahmado A, Sugano E, Allen AE, Lawrence JM, Tomita H, Coffey PJ, Vugler AA (2010) Dissecting a role for melanopsin in behavioural light aversion reveals a response independent of conventional photoreception. PLoS One 5:e15009.

Semo M, Gias C, Ahmado A, Vugler A (2014) A role for the ciliary marginal zone in the melanopsin-dependent intrinsic pupillary light reflex. Exp Eye Res 119:8–18.

Semo M, Lupi D, Peirson SN, Butler JN, Foster RG (2003a) Light-induced c-fos in melanopsin retinal ganglion cells of young and aged rodless/coneless (rd/rd cl) mice. Eur J Neurosci 18:3007–3017.

Semo M, Peirson S, Lupi D, Lucas RJ, Jeffery G, Foster RG (2003b) Melanopsin retinal ganglion cells and the maintenance of circadian and pupillary responses to light in aged rodless/coneless (rd/rd cl) mice. Eur J Neurosci 17:1793–1801.

Sherry DM, Wang MM, Bates J, Frishman LJ (2003) Expression of vesicular glutamate transporter 1 in the mouse retina reveals temporal ordering in development of rod vs. cone and ON vs. OFF circuits. J Comp Neurol 465:480–498.

Smallwood PM, Olveczky BP, Williams GL, Jacobs GH, Reese BE, Meister M, Nathans J (2003) Genetically engineered mice with an additional class of cone photoreceptors: implications for the evolution of color vision. Proc Natl Acad Sci U S A 100:11706–11711.

Soucy E, Wang Y, Nirenberg S, Nathans J, Meister M (1998) A novel signaling pathway from rod photoreceptors to ganglion cells in mammalian retina. Neuron 21:481–493.

Strettoi E, Porciatti V, Falsini B, Pignatelli V, Rossi C (2002) Morphological and functional abnormalities in the inner retina of the rd/rd mouse. J Neurosci 22:5492–5504.

Takada Y, Fariss RN, Tanikawa A, Zeng Y, Carper D, Bush R, Sieving PA (2004) A retinal neuronal developmental wave of retinoschisin expression begins in ganglion cells during layer formation. Invest Ophthalmol Vis Sci 45:3302–3312.

Thyagarajan S, van Wyk M, Lehmann K, Lowel S, Feng G, Wassle H (2010) Visual function in mice with photoreceptor degeneration and transgenic expression of channelrhodopsin 2 in ganglion cells. J Neurosci 30:8745–8758.

Tu DC, Batten ML, Palczewski K, Van Gelder RN (2004) Nonvisual photoreception in the chick iris. Science 306:129–131.

Valente-Soriano F, García-Ayuso D, Ortín-Martínez A, Jiménez-López M, Galindo-Romero C, Villegas-Pérez M, Agudo-Barriuso M, Vugler A, Vidal-Sanz M (2014) Distribution of melanopsin positive neurons in pigmented and albino mice: evidence for melanopsin interneurons in the mouse retina. Front Neuroanat 8:1–17.

Vugler AA (2010) Progress toward the maintenance and repair of degenerating retinal circuitry. Retina 30:983–1001.

Vugler AA, Semo M, Joseph A, Jeffery G (2008) Survival and remodeling of melanopsin cells during retinal dystrophy. Vis Neurosci 25:125–138.

Wang S, Villegas-Perez MP, Vidal-Sanz M, Lund RD (2000) Progressive optic axon dystrophy and vascular changes in rd mice. Invest Ophthalmol Vis Sci 41:537–545.

Weng S, Estevez ME, Berson DM (2013) Mouse ganglion-cell photoreceptors are driven by the most sensitive rod pathway and by both types of cones. PLoS One 8:e66480.

Williams RW, Strom RC, Rice DS, Goldowitz D (1996) Genetic and environmental control of variation in retinal ganglion cell number in mice. J Neurosci 16:7193–7205.

Xue T, Do MT, Riccio A, Jiang Z, Hsieh J, Wang HC, Merbs SL, Welsbie DS, Yoshioka T, Weissgerber P, Stolz S, Flockerzi V, Freichel M, Simon MI, Clapham DE, Yau KW (2011) Melanopsin signalling in mammalian iris and retina. Nature 479:67–73.

Zhang DQ, Belenky MA, Sollars PJ, Pickard GE, McMahon DG (2012) Melanopsin mediates retrograde visual signaling in the retina. PLoS One 7:e42647.

APPENDIX A. SUPPLEMENTARY DATA

Supplementary data associated with this article can be found, in the online version, at http://dx.doi.org/10.1016/j.neuroscience.2014.11.044.